FABRICATION AND IN VITRO TESTING OF SYNTHETIC ARTERIAL GRAFTS

by

Ya Gao

Bachelor of Science, Beijing University of Chemical Technology, 2015

Submitted to the Graduate Faculty of

Swanson School of Engineering in partial fulfillment

of the requirements for the degree of

Master of Science

University of Pittsburgh

2017

UNIVERSITY OF PITTSBURGH

SWANSON SCHOOL OF ENGINEERING

This thesis was presented

by

Ya Gao

It was defended on

March 29, 2017

and approved by

Joseph John Mccarthy, PhD, Professor

Department of Chemical and Petroleum Engineering

Anne Robertson, PhD, Professor

Department of Mechanical Engineering and Materials Science

and Department of Bioengineering,

Thesis Advisor:

Sachin S. Velankar, PhD, Associate Professor

Department of Chemical and Petroleum Engineering

FABRICATION AND IN VITRO TESTING OF SYNTHETIC ARTERIAL GRAFTS

Ya Gao, M.S.

University of Pittsburgh, 2017

Cardiovascular diseases (CVD) is now the main cause for death around the world. One of the major treatment to it is bypass grafting using a synthetic graft or patient's own blood vessels to bypass the blocked area. However, the existing prosthetic graft for this surgery has poor long term patency, i.e. does not remain open for extended periods. The failure of existing graft is the result of platelet adhesion, which forms clots and then restricts blood flow. The purpose of this thesis is to introduce a new-generation synthetic graft which is flexible with an internal topography that changes continually due to normal pulse pressure oscillations. This thesis describes fabrication of such grafts, quantifies their expansion and contraction under pulsatile flow, and tests whether it reduces bio-fouling. The thesis also discusses the design strategy for such grafts so that they can work under certain pressure with a controlled deformation. Finally, we validate grafts with whole blood and platelet rich plasma to find out whether they reduce biofouling in vitro, also as a prelude to animal experiments.

TABLE OF CONTENTS

LIST OF TABLES

LIST OF FIGURES

PREFACE

First, I would like to thank my advisor Dr. Sachin Velankar. Door to his office was always open whenever I ran into a problem or had a question regarding to my research. Thanks to him, I could finish this research work and my thesis.

I would also like to thank Dr. Luka Pocivavsek, for providing me with all the guidance and help I asked.

I am also grateful to Prof. Robert Parker, for sparing his time on helping me solving problems and building a model.

Dr. Ipsita Banerjee, for letting me use her lab. And Tommy Richardson, for all the help and advice.

I would also like to thank Joseph Pugar and Nicholas Strauch for their kindly assistant. Without them, the experiments would not be so successful.

Dr. François Tchi-Ho Yu, for providing me with all the necessary facilities for the research.

Dr. Sang-Ho Ye, for his generous suggestions.

All my group member and my friends for inspiring me and comforting me when I came across with problems.

Last but not the least, I would like to thank my parents for consistently supporting me and caring me throughout studying in united states and my life in general.

1.0 INTRODUCTION

Obesity, diabetes and smoking are leading to an increase in the population suffering from cardiovascular diseases (CVD) around the world, which causes more than 30% of worldwide deaths. [1]–[4]. Coronary and peripheral vascular diseases are very common among all types of CVDS. Coronary artery disease (CAD) refers to a plaque builds up inside the coronary arteries,[5], [6] and peripheral artery disease (PAD) is plaque inside arteries which reduces the supplement of blood flow for limbs and organs.[7], [8]

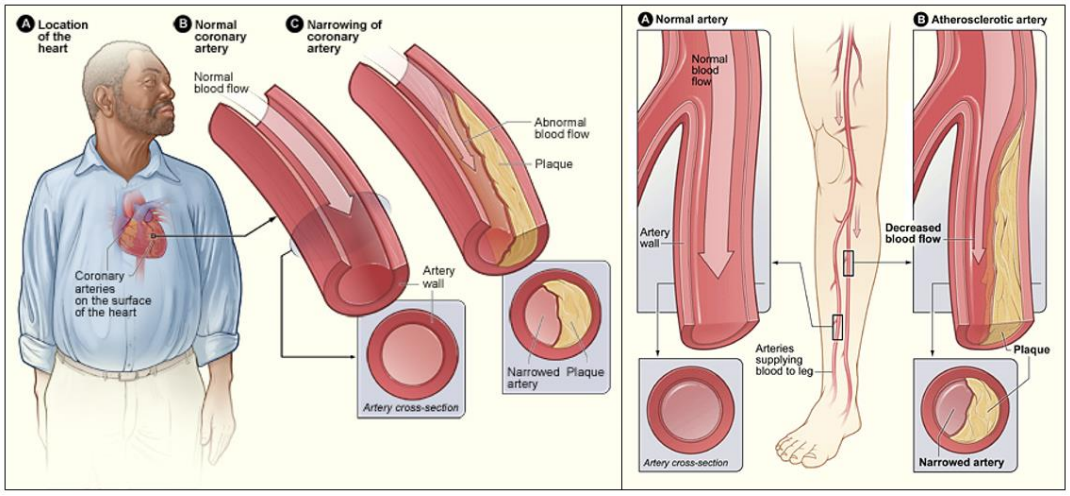

Figure 1-1 Diagrams of CAD (left) and PAD (right) [6], [7]

As shown in Figure 1-1, there are blockages in blood vessel, which lead to insufficient blood supply downstream of the blockage. There are many treatment to this kind of diseases, such as developing a heart-healthy lifestyle and medication.[5], [8]–[10] However for many patients,

especially older ones with serious conditions, drug treatment usually has limited effect. [11] Bypass grafting is always considered as a general surgery to such blockages. Figure 1-2 shows a schematic of an above-knee bypass grafting. A conduit is implanted which bypasses the blocked artery, to ensure the supply of blood at downstream.

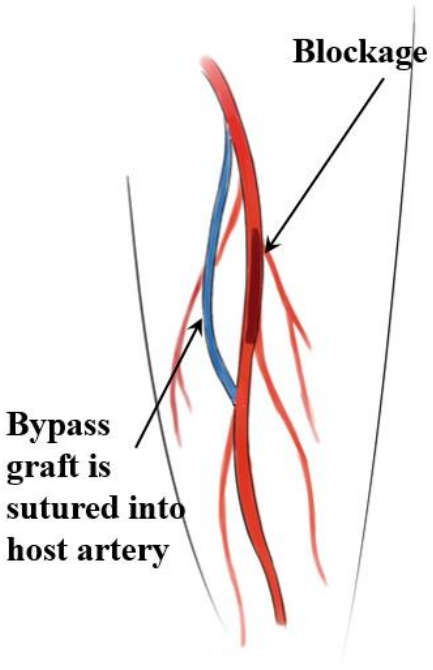

Figure 1-2 Bypass grafting for PAD [12]

Autologous grafts, i.e. blood vessels taken from the same patient, are the "ideal" material, due to its great accessibility (i.e. ease of use) and superior patency (i.e. ability to remain open). [13], [14] Patency is a very important factor when talking about bypass graft, it is the blood flow rate of normal part and blocked part (or where bypass graft locates) and normal part. Compared with synthetic graft which only maintain its patency of 39%, vein grafts remain a patency of 74% after 5 years.[15] However, roughly one third of patients, especially from the elderly population, do not have viable, autologous blood vessels, since they may have other vascular diseases or

their physical condition is not good enough to support such graft.[16], [17] Moreover, harvesting the patient's vessels requires additional surgery, which can itself cause complications given that the patients (especially diabetics) suffer from poor wound healing. Finally, in some patients, the most desirable autologous vessels may already have been used up in previous bypass surgeries. For all these reasons, artificial grafts are desirable, and various synthetic grafts are available, made of materials such as woven polyethylene terephthalate (PET) (also known as Dacron®), and expanded polytetrafluoroethylene (ePTFE).[18]–[20] Due to the lack of biocompatibility at the inner surface of these exiting grafts, thrombus forms on these surface, which leading to high failure rate of synthetic grafts.[21] These materials are very rigid compared to their host arteries, and their patency is poor when they are in low-flow areas, like below-knee, or with a small diameter (less than 6mm).[22]–[24] Some studies show that they tend to keep a good patency above-knee in large diameter surgeries, but patency is still far from satisfactory, and they also increase the risk of infection. [15], [25] Over the past 40 years, surgeons have tried to develop a durable prosthetic graft, most importantly one that maintains a high-patency even when small diameter is needed. Some strategies to improve vascular grafts are to coat grafts with anti-thrombotic drugs, or to develop other polymers for grafts. [26] However, many challenges remain.

Here we seek to develop prosthetic grafts that mimic one key feature of natural arteries. The luminal surface of muscular artery is always folded and form ridges hundreds of microns long. An in vitro study carried by Greensmith and Duling shows that the luminal surface of four muscular vascular with different initial diameter, they go to smooth and un-wrinkled when expanded, and back to folded when they get relaxed (shown in Figure 1-3). [27] This change in internal topography with pressure is a key feature that is missing in existing synthetic grafts. The

arterioles examined by Greensmith and Duling had a diameter range from 70 to 92 μm. However, it must be emphasized that for arteries with a larger diameter (such the arteries involved in typical vascular bypass surgeries), there is no physiological evidence for wrinkling-unwrinkling with diameter changes. Nevertheless, they are heavily wrinkled when relaxed, and hence changes in surface texture with changes in diameter may happen in those cases as well.

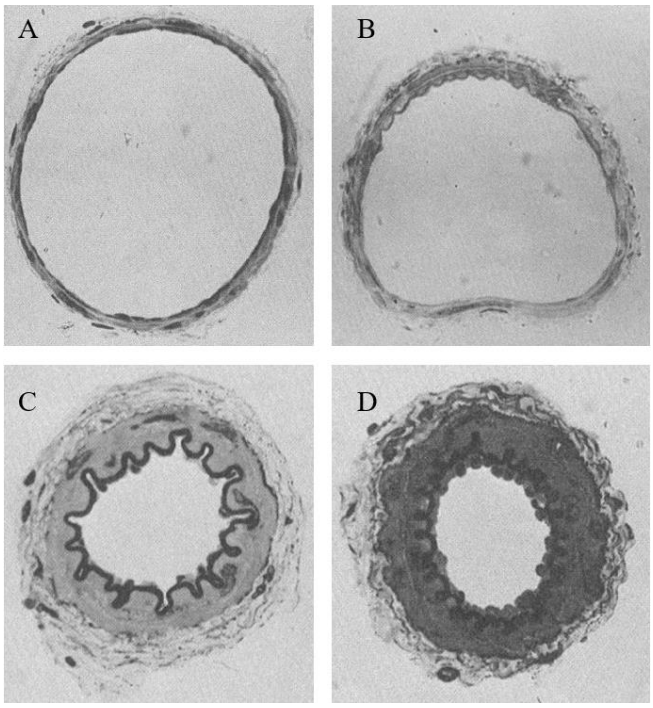

Figure 1-3 Four cross-section of arterioles at different expansion. A.125% of its original diameter (84 μm); B. 111% of 80 μm; C.72% of 92 μm; D. 34% of 70 μm[27]

The idea being followed in this research is to build a graft to mimic this dynamic in which the inner surface is flat under expansion (high pressure), and wrinkled under constriction (low pressure). With this dynamic, surface biofouling may be avoided, thus allowing grafts to maintain patency for long time. If successful, this strategy could be applied to many existing polymers suitable for implanting in human body i.e. it is not dependent on any specific material chemistry.

2.0 BACKGROUND AND PREVIUOUS RESEARCH

In this chapter, we will first describe some basic physics of wrinkling of thin films on soft substrate. It is the phenomenon that we exploit to create grafts with desired topography. Then previous research is reviewed. By this research, experiments are conducted to prove the hypothesis, and the different sizes of wavelength are also studied, which lays a foundation for future research.

2.1 THIN FILM WRINKLING ON SOFT SUBSTRATES

When a thin and stiff elastic film is attached to a pre-stretched softer elastic layer, it will buckle after the pre-stretch is removed (Figure 2-1). At its simplest, process can be regarded as minimizing the total elastic energy in these two layers, which is a sum of the bending energy of the stiff film, and the compression/stretching energy of the soft layer. [28]

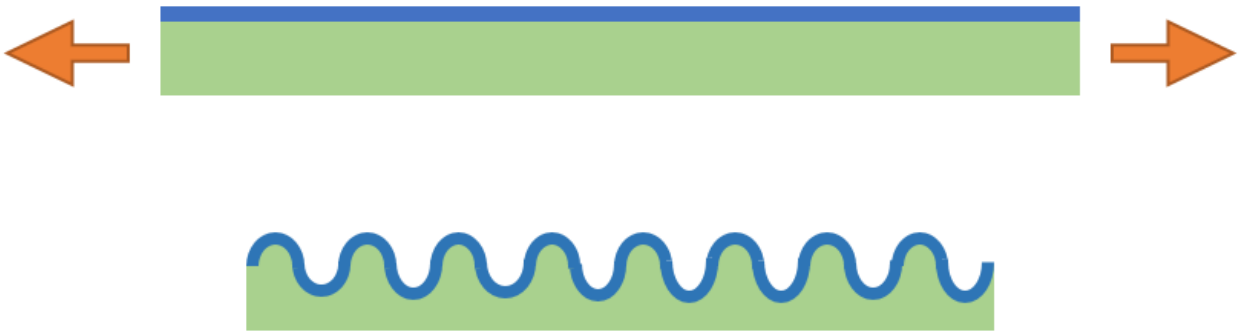

Figure 2-1 Schematic of wrinkling formation in a bilayer system

The central hypothesis of this research is that repeating a cycle of wrinkling and un-wrinkling could detach a fouling layer that sticks on the surface of the stiff film. Based on this, we develop the idea of a synthetic arterial graft composed of a multi-layered system, whose surface could be un-wrinkled when it is stretched and wrinkled when allowed to relax. This repeated smooth-wrinkle process is expected to reduce adhesion of blood clots that foul the surface. The driving force for the stretching will be the pressure drop between systole and diastole blood pressure. As shown in Figure 2-2, a and b, the inner surface will be flattened and expanded under systole (high) blood pressure (150~mmHg). Figure 2-2, c and d show the inner surface will wrinkle and shrink under diastole (low) blood pressure (60~mmHg). The range of pressure mimics cardiovascular loads. Through this process, we hypothesize that surface adhesion can be reduced greatly, and an anti-biofouling inner surface may be achieved.

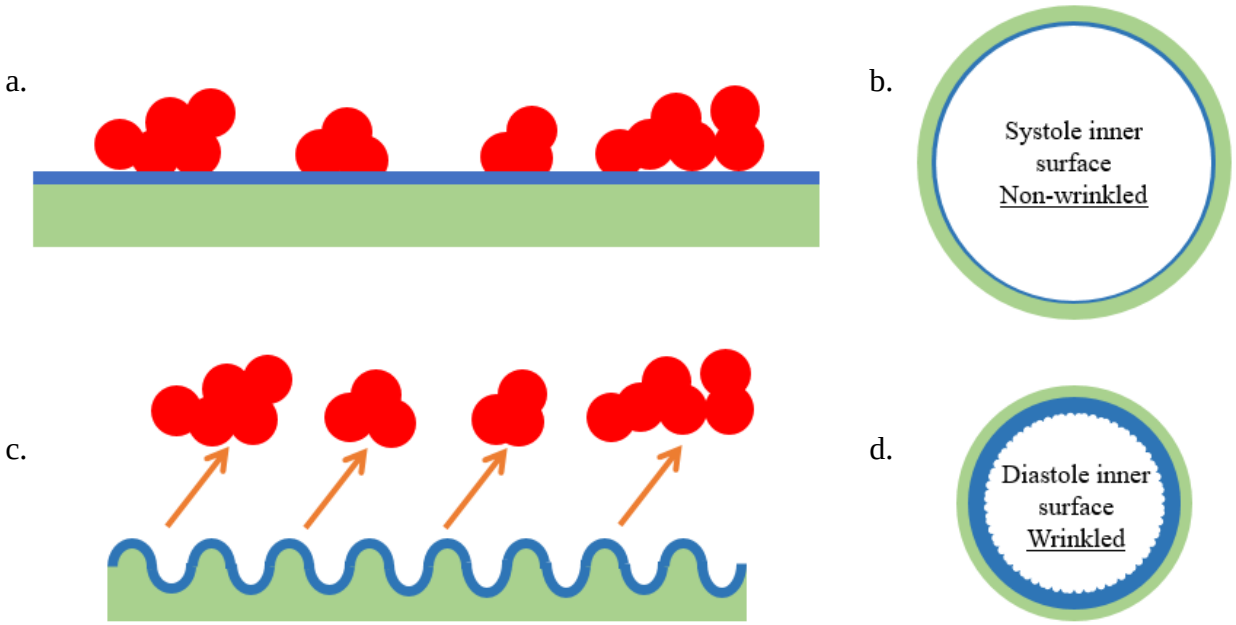

Figure 2-2 Schematic of inner surface under different pressure, and how a change in surface topography induces anti-fouling

2.2 PREVIOUS PROOF-OF-CONCEPT EXPERIMENTS

The basic idea of Figure 2-2 was validated in previous research by Dr. Luka Pocivavsek and Mr. Joseph Pugar. Flat-surface samples and wrinkled samples, with a wavelength of 50μm, were constructed by Polydimethylsilozane (PDMS). A bio-reactors were built which allow reversible wrinkling and un-wrinkling surface. Its schematic is shown in Figure 2-3. In this schematic, two black blocks are silicone actuator bases, the arched surfaces are samples adhered to the actuator base along its edges, the red colored part is where fresh ovine blood is located in the validation experiment. The driven force here is water pump underneath the test surface, alternately inflated between the actuated base and the other side of the sample, which balloons the sample to flatten

the test surface. Test surfaces were covered by fresh ovine blood at 37 ℃ for 90 minutes with actuation every 5 seconds.

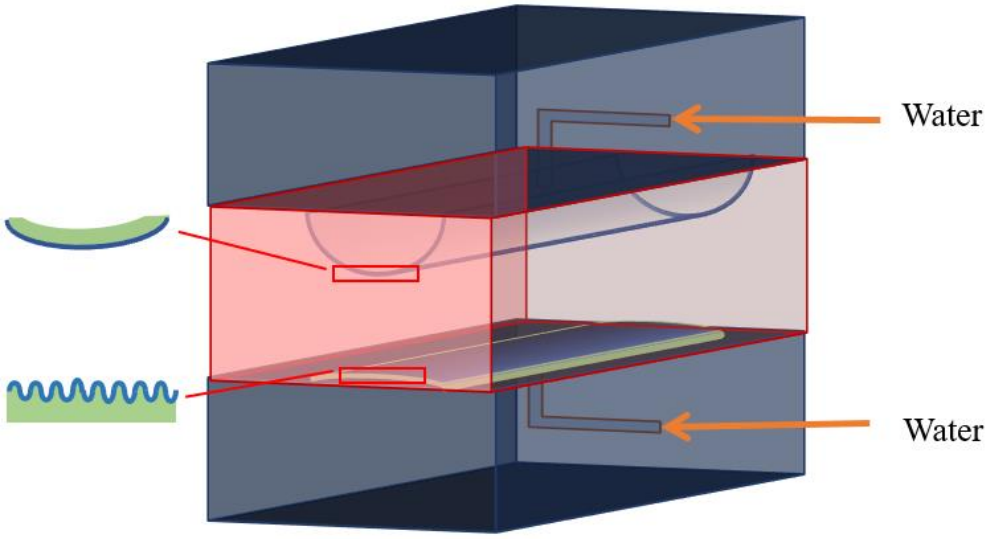

Figure 2-3 Schematic of a bio-reactor

Samples were observed by Scanning Electron Microscopy (SEM) and quantified by Lactate dehydrogenase (LDH) assay for platelet adhesion and its density. For the non-actuated controls, the surfaces were submerged in fresh ovine blood, and rocked for 90 minutes' incubation. By observing the non-actuated and actuated surfaces from SEM, it was found that actuated surfaces reduced adhesion greatly. The non-actuated wrinkled sample got the most platelet deposition due to its high surface area, non-actuated flat sample had the second-highest level of deposition on its surface. From the data gained by LDH assay, it was found that the actuated wrinkled surface decreased platelet adhesion nearly 97%. These results (which are a part of a paper to be submitted by Dr. Pocivavsek) strongly support the hypothesis (Figure 2-2) that a smooth-wrinkle transition reduces biofouling. If a similar idea can be implemented in a cylindrical geometry, then prosthetic grafts based on this principle of anti-fouling based on topographic actuation could be obtained.

2.3 THE EFFECT OF WAVELENGTH

Previous research by Dr. Pocivavsek also examined how the wavelength affects platelet adhesion. Geometries for the following experiments were all constructed by silicone-based crosslinked elastomers with specific curing agents, which are GI-245 (soft layer) and XIAMETER® RTV-4136-M (film). As shown in Figure 2-4, these multi-layer systems were first made flat in a rectangular shape, and then rolled in to a cylinder with 10cm in length and 6 mm in diameter. The seam was sutured together with 6-0 polypropylene suture, then sealed with GI-245 at a very low thickness to prevent leaking.

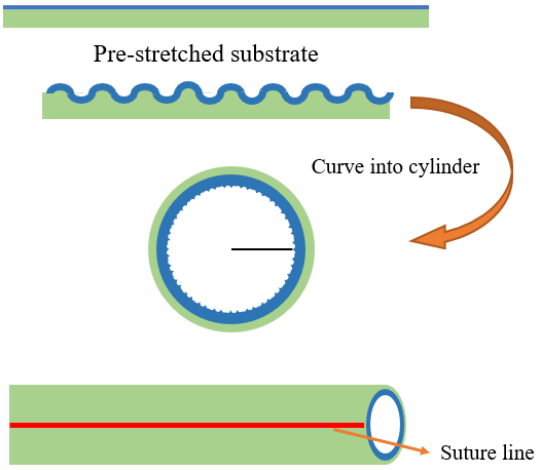

Figure 2-4 Schematic of constructing 1st generation graft

To get actuation for these samples, they were sealed at two ends with a 5fr vascular access catheter (5fr indicates that the outer diameter of tis catheter is 1.667mm) insert inside (its tip is 1mm away from the nearest cylinder end). Blood flow was output via a syringe pump, designed to provide a 2-3mL of blood at a frequency of 0.05Hz (Figure 2-5). Instead of ovine blood, whole blood provided by a healthy human was used immediately after collection. For every sample, syringe pumps were incubated at 37 ℃, and actuated for 90 minutes.

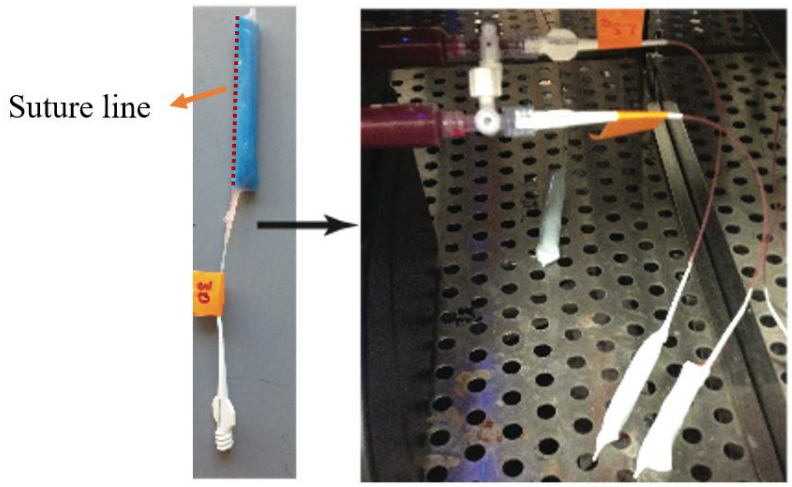

Figure 2-5 Sealed sample and how it was connected with syringe pump

Typical graft structures were tested, one with a flat luminal surface, and three with different size of wavelength. They include one graft with a very large wavelength (λ = 1000 μm), one with a medium wavelength (λ = 250 μm), and the last one has a very small wavelength, approximately λ = 80 μm. Platelet deposition of all four were analyzed by LDH assay after blood exposure. Here, platelet density on the surface is indicated by ρ with a unit of platelet/mm2.

The suture line showed significant clot formation in all samples and hence it was ignored. Thus, the sutureless half was studied. Based on the data collected by LDH assay, actuation was found to decrease platelet deposition (ρ) with a trend toward significantly decreased adhesion with smaller wavelength. On the other hand, there was no significant difference observed between flat and large wavelength samples, those with $\lambda \geq$ 1000 μm. Also, by comparing the platelet deposition on sample with a wavelength of 1000 μm, 250 μm and 80 μm, showed a clear and statistically significant decrease in platelet adhesion with decreasing wavelength.

2.4 DESIGN OF MULTI-LAYER SYSTEM

As mentioned above, early samples prepared by Dr. Luka Pocivavsek were fabricated flat, and then sutured together to form a cylindrical geometry to mimic artery. However, the suture line introduces highly thrombogenic area which clots heavily and hence a new method to prepare cylindrical samples without suturing is necessary. In this method, we follow a strategy of creating a tubular sample in which a thin stiff cylindrical film is attached to the inside of an inflated soft cylindrical tube. Upon relaxing the inflation, the soft tube shrinks, thus inducing wrinkles on the inner surface. This is illustrated in Figure 2-6 a and b. Detailed description will be given in next chapter.

As discussed above, wavelength of graft greatly impacts the amount of platelet adhesion. Since we realize the wrinkles using the compression-induced buckling of a thin film on a soft substrate, we must examine how wavelength can be tuned in that situation. The wrinkle wavelength (λ) is related to the thickness (h_f) of stiff membrane and the mechanical properties of two materials, which is described by scaling law [29]–[31]:

$$\lambda = 2 \cdot \pi \cdot h_f \cdot \left(\frac{\overline{E_f}}{3\overline{E_s}}\right)^{\frac{1}{3}} \qquad \text{Equation 2-1}$$

E_f and E_s are the Young's Moduli of film and substrate respectively and $\overline{\mathrm{E}} = E/(1-\nu^2)$, where ν is the Poisson's ratio, which is 0.5. The subscripts f and s refer to the stiff film and soft substrate, respectively. Based on the data collected by Mr. Joseph Pugar, the modulus for the stiff layer and substrate layer respectively are $\mathrm{E}_f = 2.7\mathrm{MPa}$ and $\mathrm{E}_s = 27.7\,\mathrm{kPa}$. With the desired wavelengths (λ), the needed thickness (h_f) can be estimated easily. The pre-strain of the

substrate also affects the buckling phenomenon, but to a first approximation, it affects not the wavelength but the amplitude[29]:

$$A = h_f \left(\frac{\varepsilon_0}{\varepsilon_c} - 1\right)^{\frac{1}{2}} \qquad \text{Equation 2-2}$$

where ε_0 is the strain, and ε_c refers to critical strain for wrinkle formation, calculated by $\varepsilon_0 = \frac{1}{4}\left(\frac{3\overline{E_s}}{\overline{E_f}}\right)^{\frac{2}{3}}$.

Based on the conclusion from chapter 2.3, the desired wavelength is between 100 and 150 microns. Applying in to equation 2-1, desired thickness (h_{f-d}) could be got easily, which is in a range of 5-10 microns.

In summary, the approach to graft design is to select the film and the substrate materials first, and then estimate the film thickness from the desired wavelength. The thickness of the softer layer is then selected based on other considerations, e.g. ease of suturing or manufacturing.

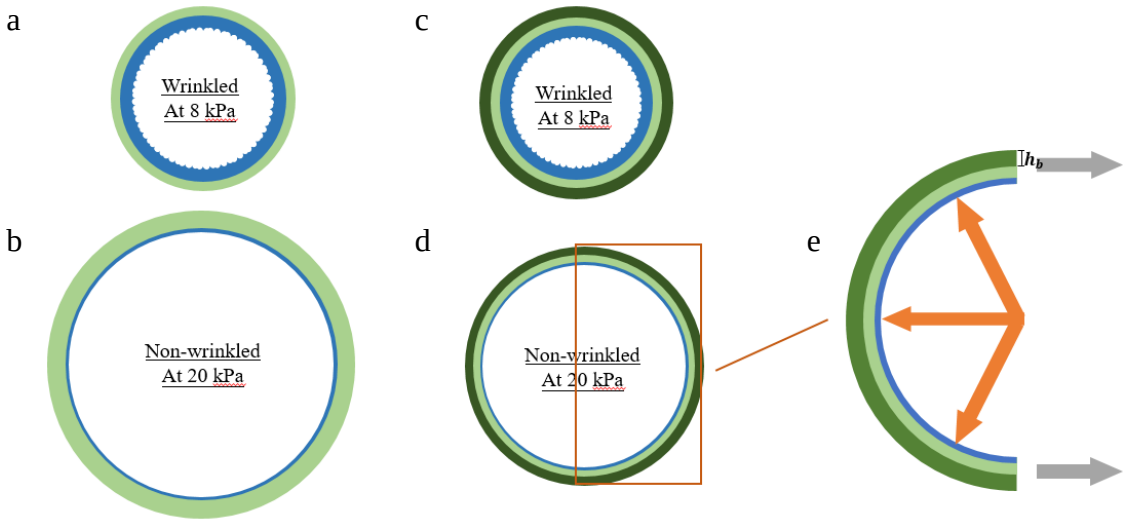

Figure 2-6 a-d are the schematic of graft with/without build-up layer at certain pressure; e is the stress analysis diagram when graft expanded at 20 kPa

The materials to be used for the fabrication will be discussed later, however we found that at the desired pressure around 150 mmHg (20kPa), the cylinders expanded excessively as will be shown later in Figure 4-4. Accordingly, a stiffening layer was added to the outside of these two layers. As shown in Figure 2-6, a comparison of a-b vs c-d indicates how the stiffening -up layer changes the deformation of grafts. Figure 2-6 e, shows an elementary stress analysis of graft, orange arrows indicate for the inner pressure, which leads to the expansion of graft. Grey arrows are counter-acting forces in the cylinder walls (hoop stress) due to the expansion. During the fabrication procedure, the stiff film and soft substrate are made first to ensure the right wavelength is achieved, then the stiffening layer is coated to the outside of relaxed cylinder to restrict the deformation of graft under high pressure. The modulus of the stiffening material, also tested by Mr. Joseph Pugar, is E_b = 4.3MPa.

Based on the stress analysis, we can write

$$(P_H - P_L) \times D = 2 \times (E_b h_b + E_s h_s) \varepsilon \qquad \text{Equation 2-3}$$

Where, P_H and P_L refer to high and low pressure, which are 8kPa and 20kPa respectively (corresponding to systolic and diastolic pressures). D is diameter (4mm) of graft. E_b and Es are moduli of the build-up layer and the substrate, which are 4.3 MPa and 27.7 kPA respectively; h_b and h_s are thickness of these layers, and h_s is 1.2mm; ε is the expected strain, which is 0.2. Here we assume that the innermost stiff film does not contribute significantly to the hoop stress since it is both very thin, and pre-buckled.

By substituting moduli, pressure drop, initial inner diameter of 4mm, thickness of substrate, and expected strain, the desired thickness of the stiffening layer can be easily calculated, which is around 19 μm.

A typical example of our graft is shown in Figure 2-7 (fabrication is described in the next chapter). The h_f values appears to be close to 50 microns, much higher than the value of 5microns calculated from equation 2-1 above. Nevertheless, the wavelengths were still on the order of 200 microns (see Figure 2-7). Thus, for reasons that are not clear, equation 2-1 is not able to predict the observed wavelength correctly in our experiments, yet, fortunately, we are still able to realize the desired wavelengths on the inner surface of grafts.

Moreover, thickness of the stiffening (h_b) can also be estimated to be 240 microns. Once again, this is far larger than the desired value estimated from Equation 2-3. Nevertheless, such grafts gave the desired strains of a few ten percent. Once again, there reasons for the discrepancy are not clear. This will be discussed further in chapter 6.

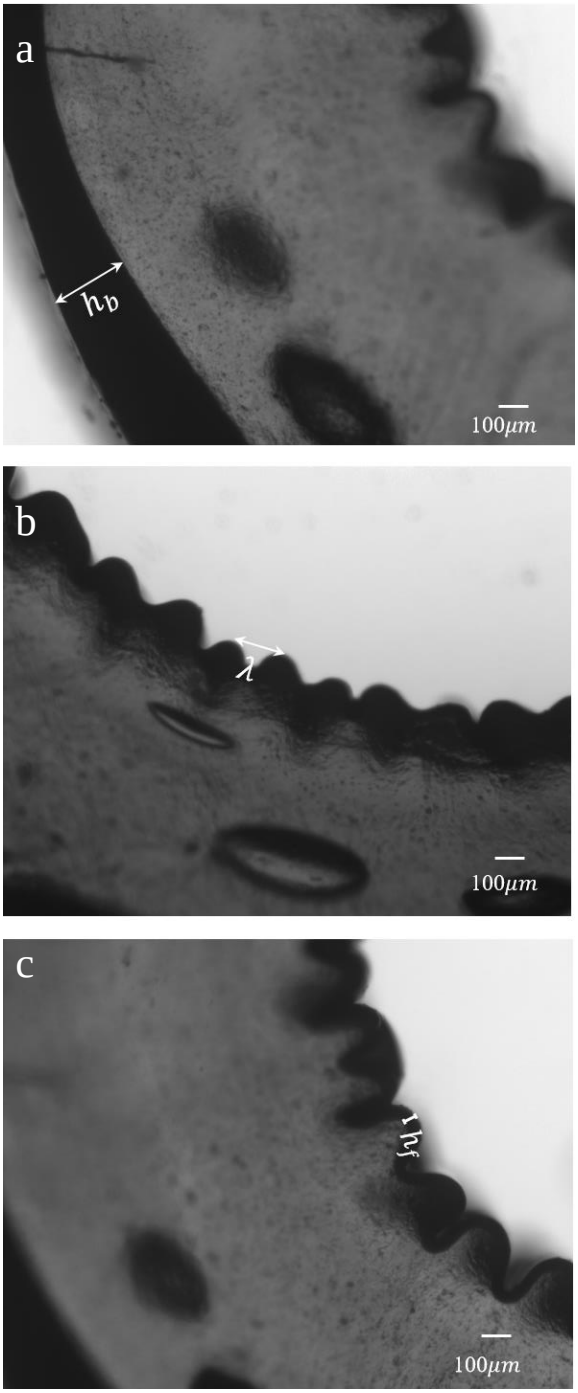

Figure 2-7 Microscopic picture of graft cross-section (a. thickness of stiffening layer; b wavelength; c thickness of film)

3.0 CONSTRUCTING METHOD – FABRICATION

To construct this cylindrical graft, the main method used is dip coating each layer, followed by bonding them together. All polymers used here are silicone-based thermoset elastomers with specific curing agents. Since silicones have high biocompatibility, good durability, flexibility and softness, these properties make it a good material to construct a vascular graft. Also, they have a good chemically adhesive with each other, no additional reaction is needed when coating them layer by layer. As judged by peeling experiments, uncured GI-245 has a good chemical adhesion on cured XIAMETER® RTV-4136-M (M-4), and uncured GI-380 shows a good curing on other silicone materials.

Figure 3-1 Texture analyzer instrument (used as dip coater)

The uniformity of thickness of grafts is crucial to their performance in experiments. To control the thickness and realize wrinkles with small wavelength, a dip coater is needed. Instead of a standard dip coater, we are using used a Texture Analyzer instrument, which can provide the controlled-speed translation needed for dip coating (Figure 3-1). An acrylic rod can be fixed on the shaft of the instrument with a metal clamp, lowered into a bath of uncured silicone, and withdrawn. In our case, the bath consists of a centrifuge tube (of 12cm in length and 1.5cm in OD) filled with the uncured silicone to be coated onto the tube. Detailed information could be

found in table 3-1. It is worth noticing that for 1st /2nd layer of GI-245, the amount of crosslinker is been doubled. For polymer precursors, solvent is added proportionally to reduce the thickness of each layer, also crosslinker usually has a lower density than polymer. However, adding solvent could extend the curing time. In this case, double the amount could reduce the viscosity of the mixer and also accelerate the curing time.

Table 3-1 Material List

Usage	Silicone-based polymer (A)	Curing agent (B)	Solvent (S)	Ratio	Diameter of rod/mm	Curing time/hour	Vendor
1st /2nd layer of GI-245	GI-245	Ultra-Fast-Curing crosslinker	Hexane/n-octane	10A:2B:2S	3	8-12	Silicones, Inc.
Membrane	M-4*	Specific crosslinker	Hexane/n-octane	10A:1B:4S	6	8-12	XIAMETER
Glue	GI-245	Standard crosslinker	None	10A:2B	-	Max. 12	Silicones, Inc.
Steady layer	GI-380	Specific crosslinker	None	10A:1B	-	8-12	Silicones, Inc.

* XIAMETER® RTV-4136-M

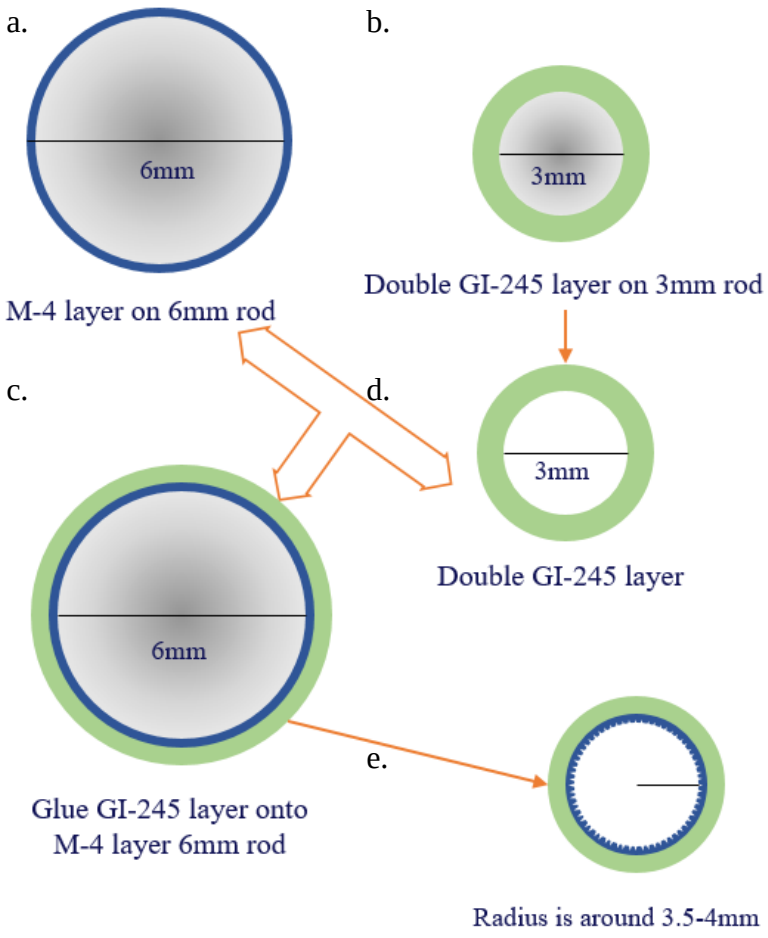

Figure 3-2 Schematic of fabrication (cross-section of every step)

The procedure is for preparing grafts, illustrated in Figure3-2, 3-3 and 3-4, is as follows:

1. Dip coating 3mm Acrylic Rods with GI-245 at a speed of 4mm/s (see Figure 3-2 a and Figure 3-3a). The ratio of base, crosslinker and solvent is 10:2:2. These rods need to be dipped twice with GI-245 with the same ratio to get the desired thickness. The crosslinker used here is the ultra-fast-curing one, and the optimal thickness of GI-245 is around 1-1.5mm after two coats (see Figure 3-4 a and b).
2. Dip coating 6mm Acrylic Rods with XIAMETER® RTV-4136-M (M-4) at a speed of 0.4 mm/s. The ratio of base, crosslinker and solvent is 10:1:4 (see Figure 3-2 b, 3-3 a and 3-4 c).
3. Remove GI-245 tubes off the rod after the second layer has cured (see Figure 3-2 c).

4. Prepare the silicone for the “glue” layer by mixing GI-245 with standard crosslinker in a ratio of 10:2, no solvent needed.
5. Take the glue and dip one of the end of the M4-coated 6mm rod (Figure 3-2 d). Then insert the 6mm rod into the GI-245 tube, which will make the GI-245 tube stretched radially, without stretching it vertically (see Figure 3-4 d).
6. After 10-12 hours to allow the glue layer to cure, remove the composite hollow cylinders off the rods (see Figure 3-2 e and Figure 3-5 a).

   After these steps, a graft with wavelength with a wavelength range from 50- 100μm will be achieved. The mean value of its wavelength is about 75μm, and) the diameter of this graft is about 5mm OD, and 3mm ID.

For the in vitro experiments, the resulting grafts were found to be too soft, i.e. they underwent large expansion and compression under the typical pressure variations between systolic and diastolic pressure. Accordingly, they were coated with one further layer of a stiff silicone, GI-380 on the outside as follows:

7. Use a syringe cap with a diameter of 4mm, fit two of them to the two ends of hollow cylinder, close to the edge. Then, dip it into the GI-380 by hand. The ratio here is 10:1. Hang the cylinder for 8-12 hours to cure (see Figure 3-5 b).

8. Repeat step 7 as needed. The number of GI-380 coats decided by the overall expected cylinder radial expansion. * Cut the cylinder off the caps.

* The following in vitro experiment shows a good result with 2 coats of GI-380, the animal experiment works better with none or one coat.

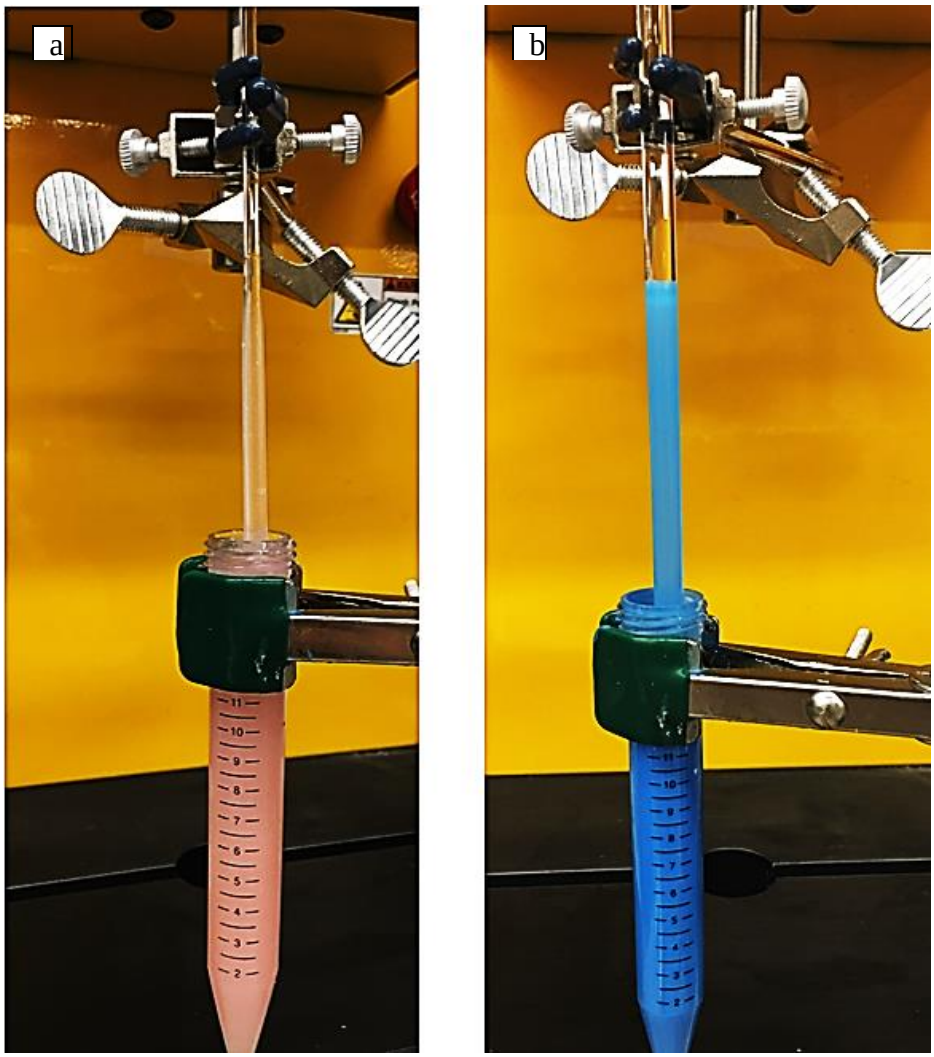

Figure 3-3 a. dip coating 3mm rod with GI-245; b. dip coating 6mm rod with M-4

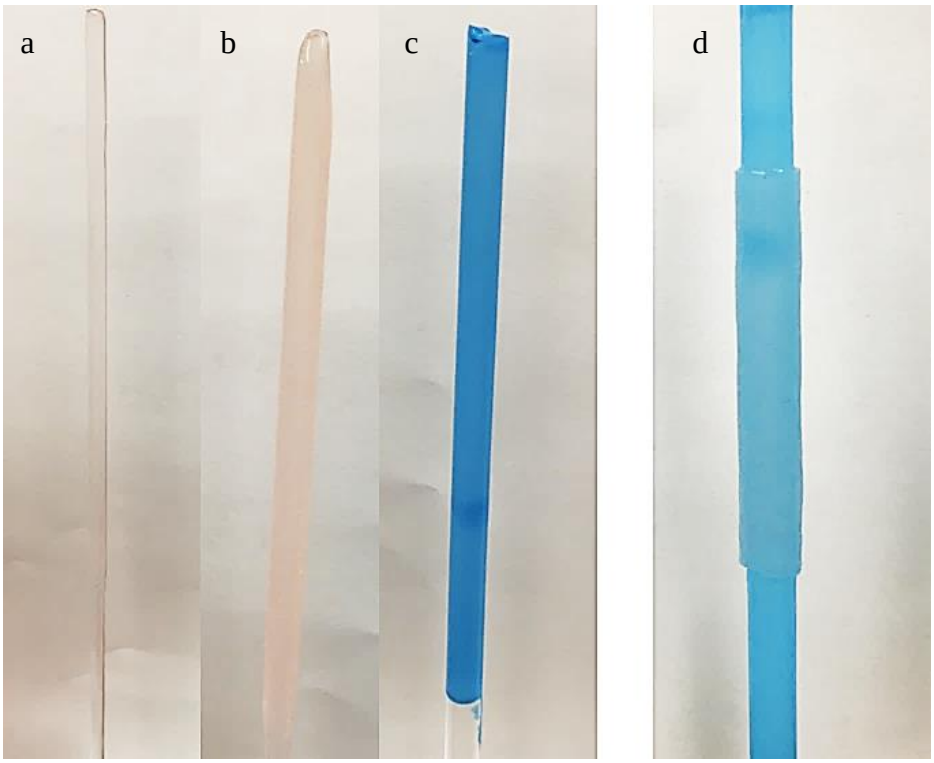

Figure 3-4 a. 3mm rod with one coat of GI-245; b. 3mm rod with two coats of GI-245; c 6mm rod with one coat of M-4; d. insert rod c in to GI-245 tube (peeled off from rod b)

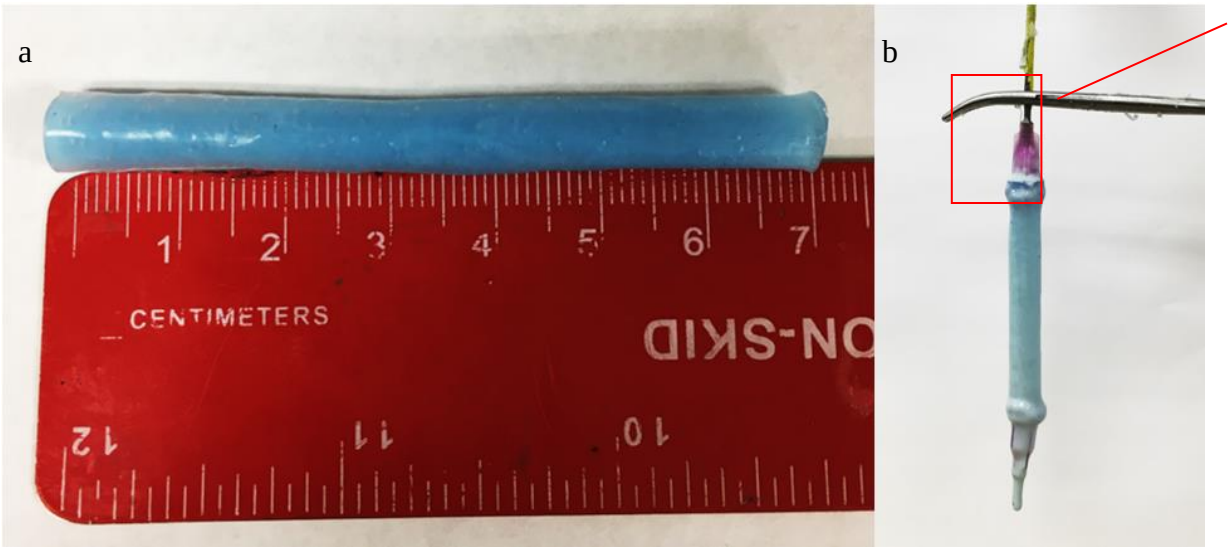

Figure 3-5 a. Original graft b. Graft coated with GI-380 (with syringe cap at each end to block GI-380 from leaking inside)

4.0 IN VITRO EXPERIMENTAL RESULTS

Before blood fouling adhesion tests, cylinders need to be tested to find out whether and how much they expand under pressures and frequencies typical of real world applications. A series of pressure experiments were conducted. To mimic the actual situation of a real blood vessel, which is pumped by the heart, a pulsatile blood pump was used. This pump is Harvard Apparatus Pulsatile Blood Pump for Rabbits. It simulates the pumping action of the heart and generates a continuous pulsatile flow. Figure 4-2 shows the actual pump, and Figure 4-1 shows a schematic of the piston chamber.

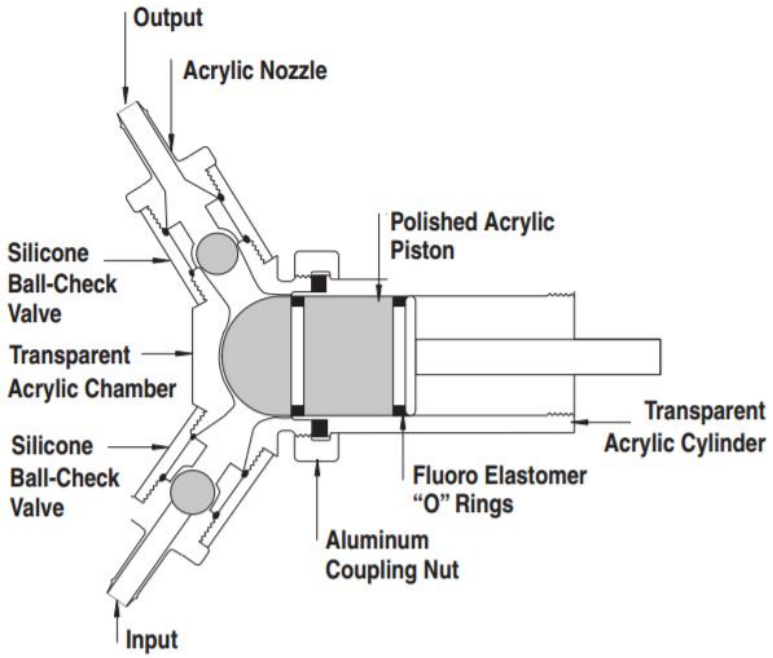

Figure 4-1 Schematic for piston chamber

As shown in Figure 4-2, the knob on the right is the rate adjustment knob, with a range from 0 to 200 strokes per min. The knob on the left adjusts the stroke volume. Volume can be read from the decal fastened to the pump cylinder, determined by the “O” ring on the piston, shown in Figure 4-1. The volume can be adjusted while the pump is running.

The piston chamber is connected to the external tubing via two one-way ball valves, one for the inlet and one for the outlet. For every stroke, the piston moves backward (to the right) first, and the negative pressure in the chamber lifts the metal ball near the entrance and liquid is sucked into the acrylic chamber. At the same time, the metal ball near the exit is forced closed. On the output stroke of the piston, the inlet ball closes whereas as the outlet opens, thus ejecting the fluid volume. Repeating the process described above, a pulsatile flow with certain rate and volume can be generated.

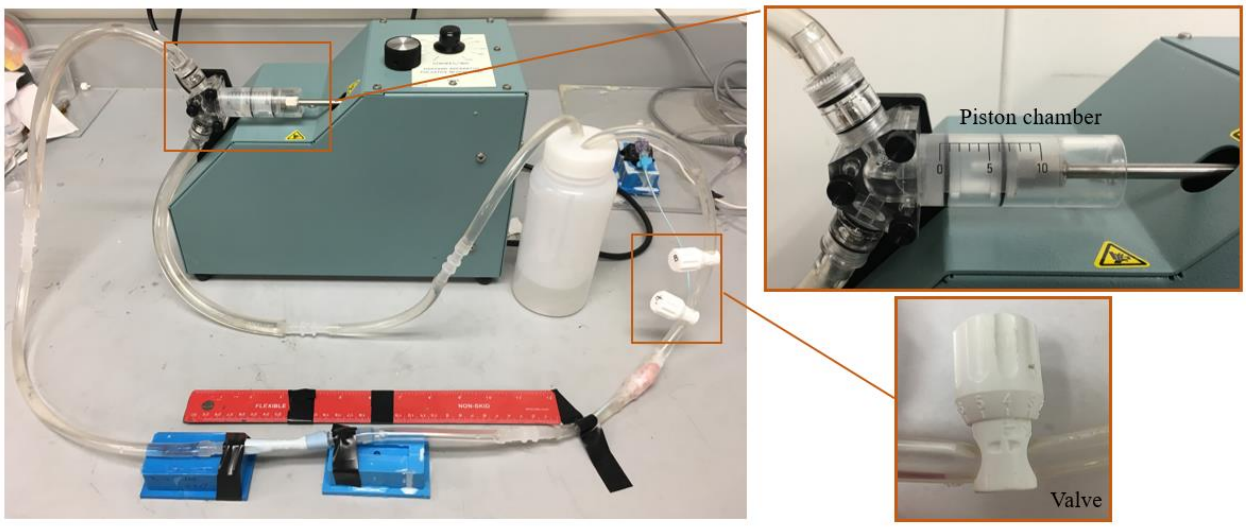

Figure 4-2 Circulatory system (run with water)

Since the actuation occurs on the luminal surface of grafts, and the thickness of the silicones under pulsatile flow is difficult to detect, a clinical vascular imaging technique called Optical Coherence Tomography (OCT) is applied. In Figure 4-3, there are two screenshots from a video

which recording the deformation of graft at the same position in vitro. The one on the left shows the cross-section of graft under low pressure, and the one on the right is the cross-section under high pressure.

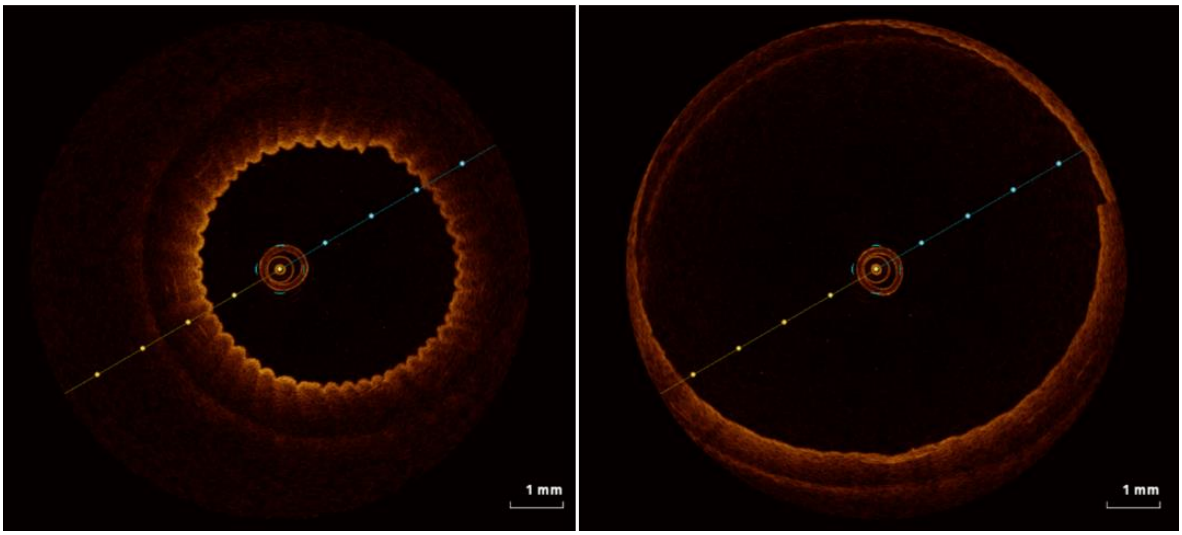

Figure 4-3 OCT of luminal surface of graft under low pressure (left) and high pressure (right)

OCT works by using low-coherence interferometry, typically employing near-infrared light which can penetrate into the scattering medium, and collecting the images along the cross-section at a high speed [32]. By moving the catheter back and forth within the tube, different locations can be imaged. The catheter (C7 DragonflyTM Imaging Catheter, LightLab) used could provide a resolution between 50-100μm.

4.1 STRATEGY FOR RESTRICTING THE DEFORMATION OF GRAFTS

Figure 4-4 illustrates the deformation behavior of a cylindrical graft at a pressure of 90mmHg in pulsatile flow at a frequency of 100 per minute. This graft has not been coated with a stiffening

layer of GI-380, and it is clear that the graft balloons up, i.e. the expansion strain is far higher than the 20% needed to drive the wrinkle-smooth transition. As explained in chapter 2.4, to restrict this expansion, a stiffer silicone, GI-380 is coated onto the outside of the graft. Its modulus is about 1000 times larger than GI-245. Note that M-4 is stiff as well, however since it has very small thickness, its effect on the gross mechanics of the tube can be ignored.

Figure 4-4 Grafts without GI-380 coating ballooned at high frequency (100/min) and loose valve setting

Equation 2-3 describes how the strain reduces as the thickness of the build-up layer increases. However, the optimal layer thickness was determined empirically. Grafts were coated externally with different number of coats of GI-380, and outer diameter at high pressure and low pressure were recorded. With the circulatory system, frequency was set to 60 and 80 strokes/min respectively, the maximum and minimum diameters recorded by video, for various number of stiffening coats, are shown in the graphical table 4-1. “LOD” and “HOD” stand for outer diameter at low pressure and outer diameter at high pressure.

From the table 4-1, for grafts without the GI-380 stiffening layer, the strain is too large even at low pressure suggesting that these grafts may not recovery to a wrinkled state even under low pressure. Grafts with 3 or 4 coats of GI-380 remain nearly static, i.e. there is not much deformation as pressure varies. Grafts dip coated with one layer of GI-380 tend to have an uneven coating, which may lead to leaking after pulsating for long time. As the number of coats of GI-380 increase, diameter of variation reduces and the pressure of variation increases. And with a tight valve setting (3.4 and 3.6), the low pressure is not much impacted of different number of GI-380 coats, high pressure goes a little bit higher than the loose setting.

Table 4-1 Comparison diameter and pressure changes for grafts with various number of GI-380 coats

Valve setting	3.4&3.6	3.6&3.6
60/min	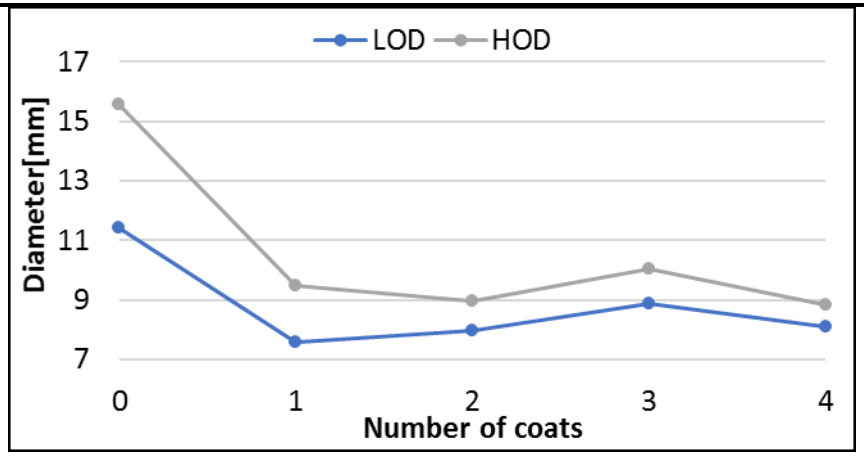	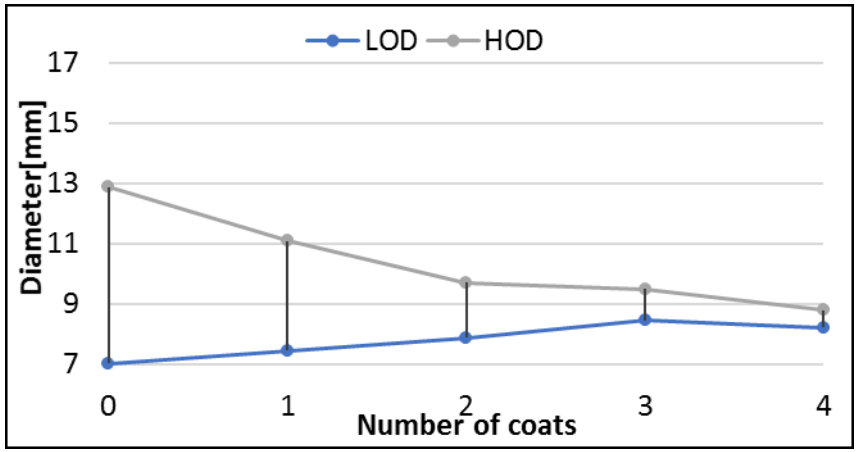
	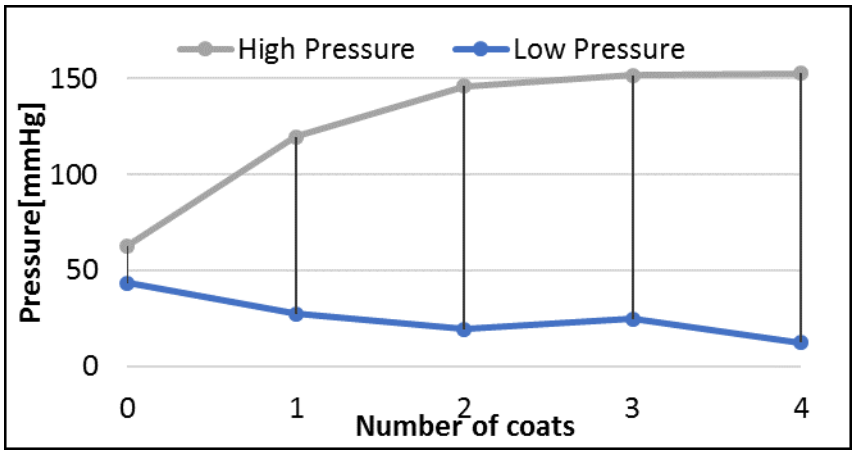	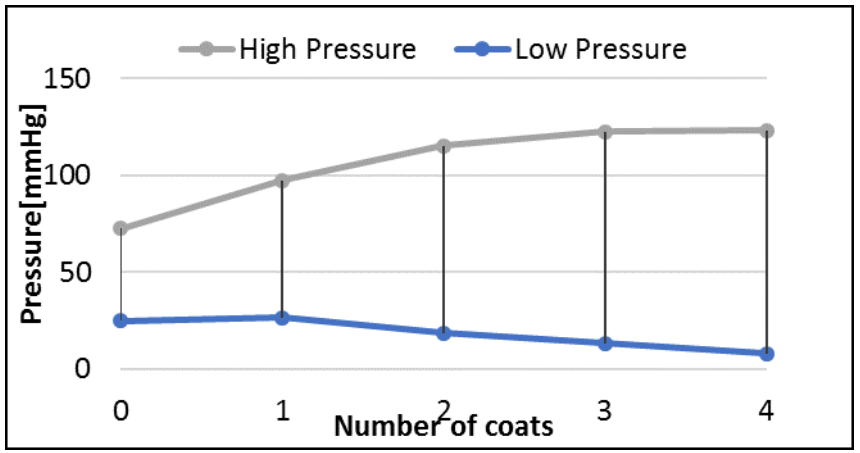

Table 4-1 (continued)

80/min

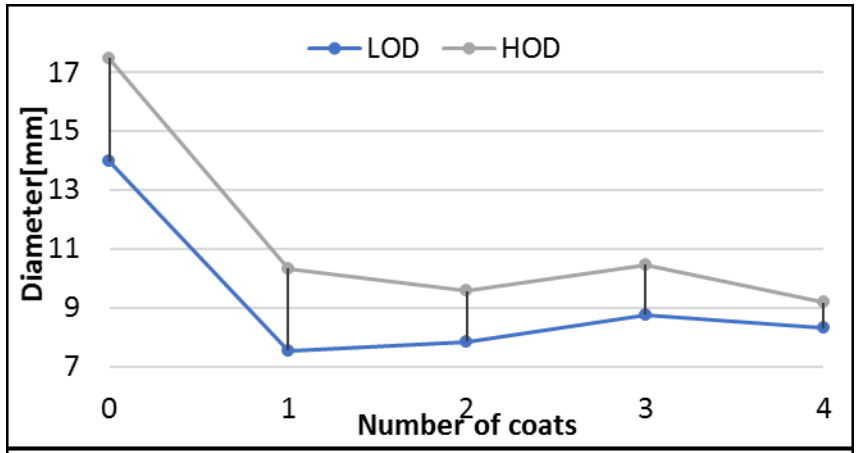

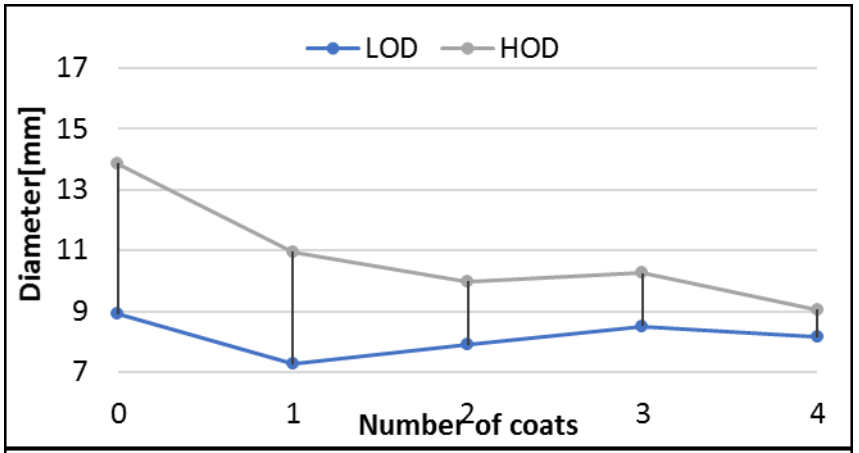

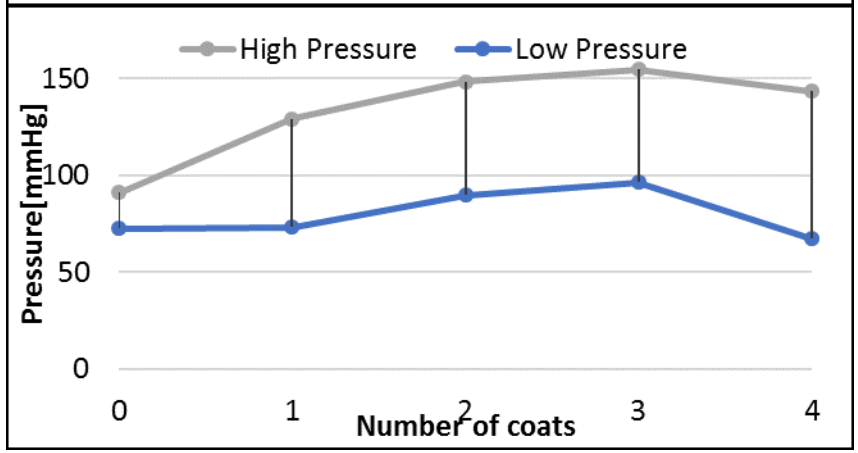

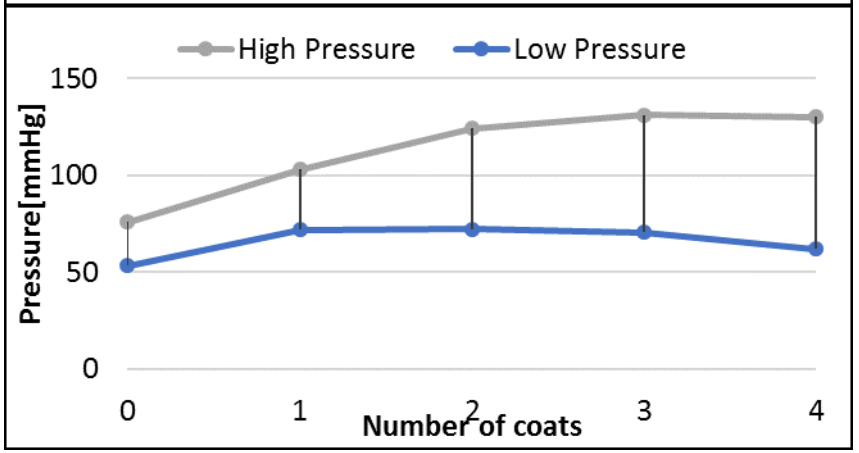

4.2 STRATEGY TO CONTROL THE PRESSURE DURING PULSATILE FLOW

Due to pulsatile flow, we could control the pressure easily by two graduated valves at the end of the outflow. By constricting the valve to some value, the Tygon tube can be squeezed. Thus, a backpressure appears, and pressure upstream (in the graft) does not drop to zero immediately after the pump finishes its forward stroke. By setting the valve to different values, the desired pressure could be achieved.

By using a pulsatile flow system shown in Figure 4-2, the cylinder is connected to the pump through Tygon tubes, and pressure is measured downstream with a pressure analyzer (Digi-Med Blood Pressure Analyzer (BPA-400)).

To characterize the pressure-expansion behavior, a series of experiments were conducted. In these experiments, grafts with 0, 1, 2, 3, 4 coats of GI-380 were pulsated at frequency of 20, 40, 60, 80, 90, 100, 110, 120. For one group, the valves are set to 3.4 and 3.6 (arbitrary graduations on the valve) separately. For another, valves are set to 3.6 and 3.6 respectively. It needs to be pointed out that a setting of 3.4 and 3.6 indicates a smaller tube diameter, i.e. a greater flow resistance. Furthermore, two valves are not necessary, in principle one is sufficient for the experiment. However, to get a finer control, two valves is applied. For every time, one graft with certain time of coats was tested, valves were set to certain value, and stroke volume for the pump was also fixed, which is 6mL. The only variable was the frequency with a range from 20 to 120 strokes/min.

Table 4-2 Pressure measurements during pulsatile flow for grafts with various stiffening layers

Valve setting	3.4&3.6	3.6&3.6
0 coat	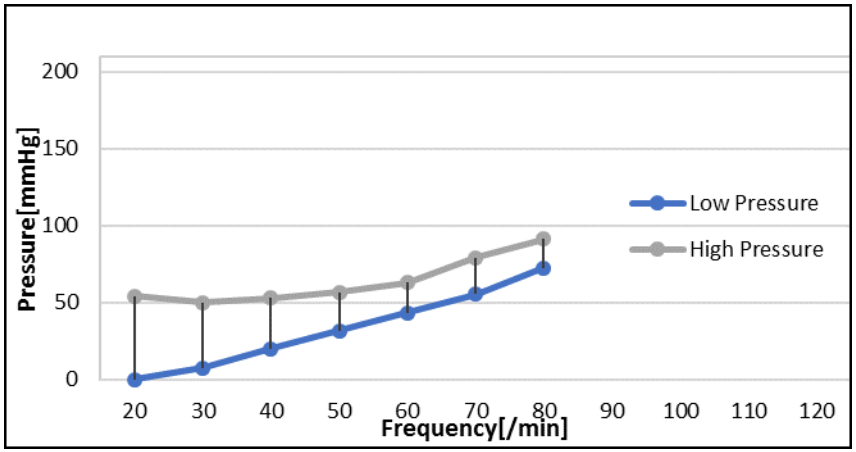	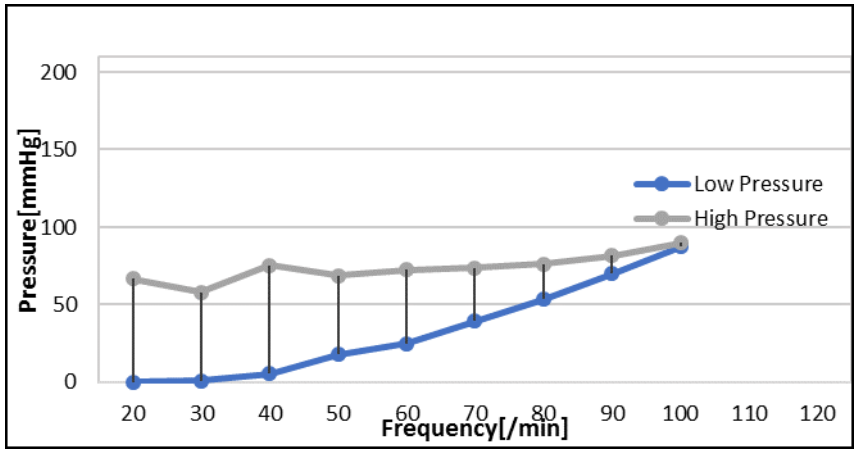
1 coat	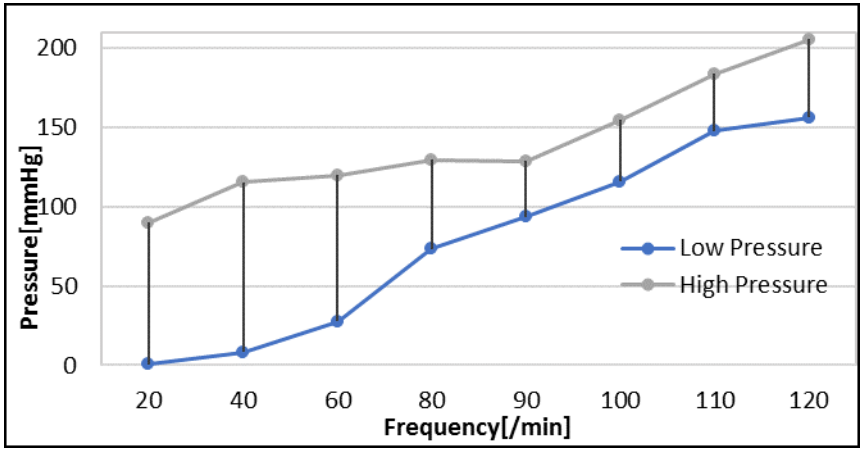	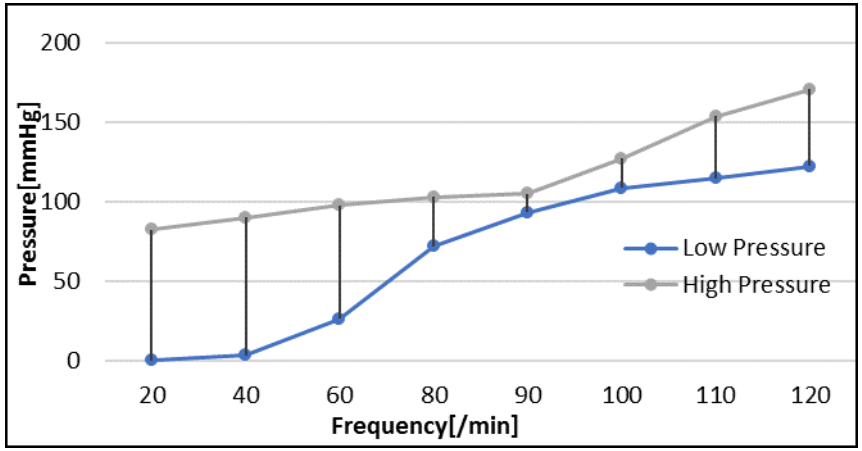

Table 4-2 (continued)

2 coats	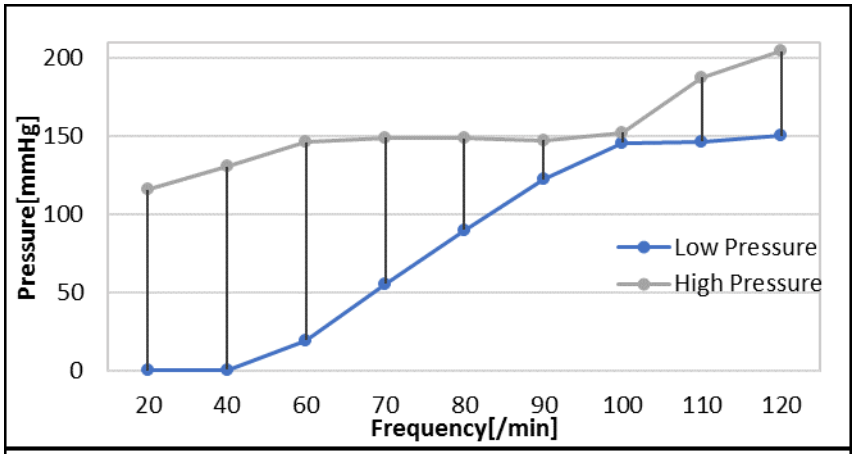	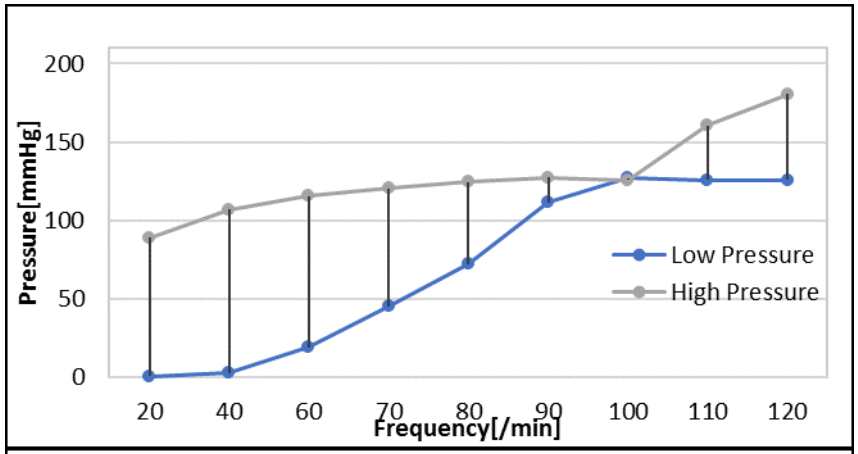
3 coats	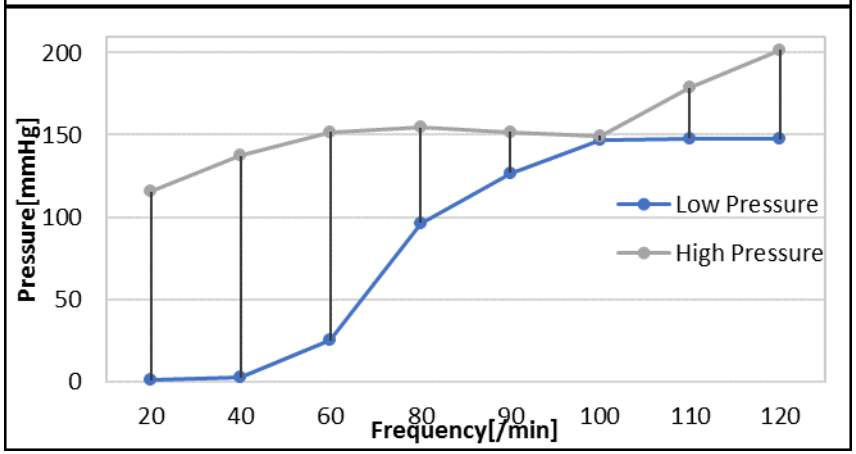	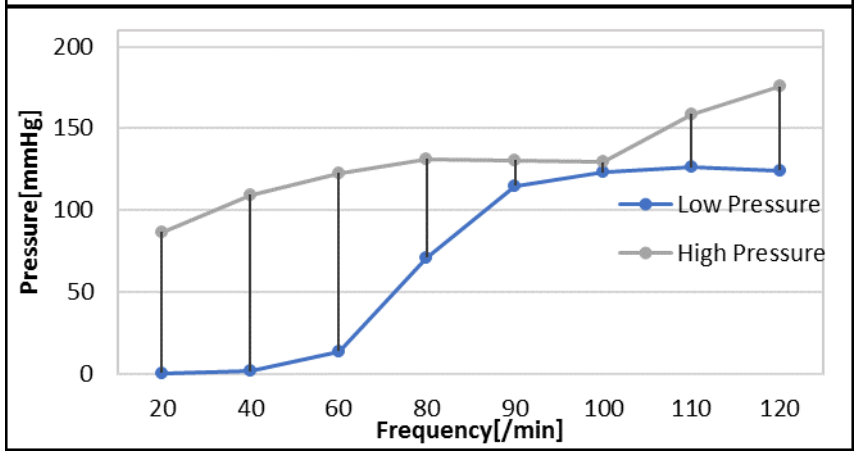

Table 4-2 (continued)

4 coats	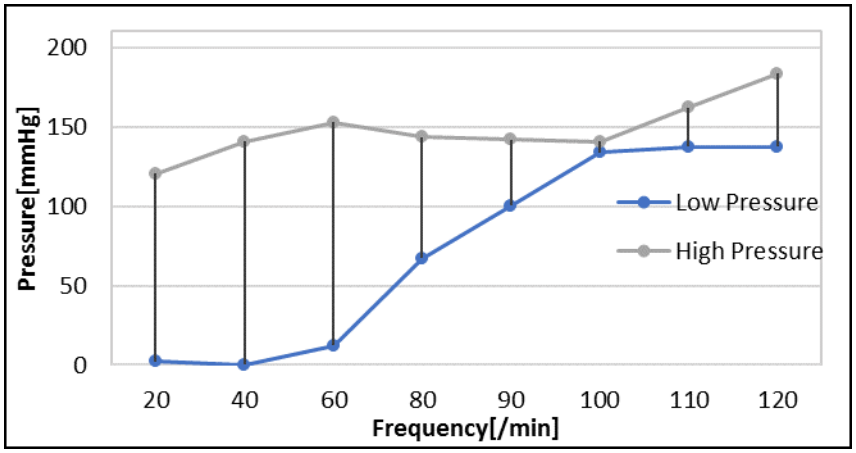	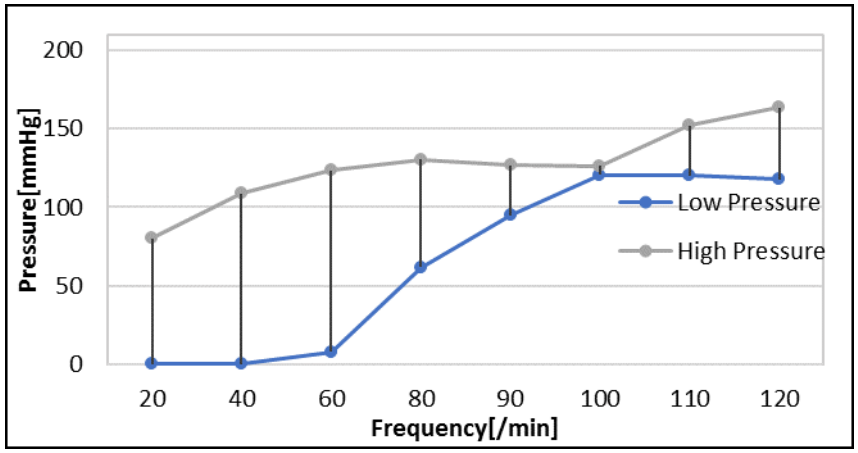

Comparing these charts above, it can be found that high pressure could increase easily with tighter tube, especially after the frequency reaches 40/min, and pressure drops to zero at low frequency which indicates a full relaxation for the graft geometries. An interesting phenomenon can also be noticed that both high pressure and low pressure reaches the same value at the frequency of 100/min in every different experiment. According to the manual of pressure analyzer, its microprocessor samples at 1000 points/sec (a very high rate), and but the panel display updates only at every 0.5 seconds (according to specification of this pressure analyzer), so it may coincide with the change pattern of pressure, which could lead to this result here. Since the panel refresh rate is quite low, time for recording and tracking data is extended to ensure similar number came up repeatedly or this number is constrained in a relative narrow range. And these experiments were carried for several times, the results turn out to keep similar to each other.

4.3 ANALYTIC MODEL

A significant oddity of the above data is the convergence of the measured pressures at some frequency. As mentioned in the above paragraph, we believe that this is an artifact of the data refresh rate of the pressure analyzer. Nevertheless, we sought to develop a simple model to judge whether, under some simplifying assumptions, such convergence could appear.

A simplified 1-dimensional model of this circulatory system (Figure 4-2) is shown in Figure 4-5. This model assumes that the main flow resistance in the entire circuit is the valve itself; the remainder of the circuit offers very little flow resistance, and hence has uniform pressure. We

also assume that the graft is the only compliant portion of the circuit, whereas the remainder of the connecting tubing undergoes negligible volume change.

The input $Q_{in}(t)$ is a square wave function, with period T. This can be written as

$$Q_{in}(t) = \begin{cases} Q_{max}, & 0 \le t < \frac{T}{3} \\ 0, & \frac{T}{3} \le t < T \end{cases} \qquad \text{Equation 4-1}$$

Here $Q_{max} = \frac{3V_c}{T}$, where V_c is stroke volume 6mL. Its plot is shown in Figure 4-5. The green block indicates a graft whose volume oscillates with time. The output flow is also a function of time $Q_{out}(t)$.

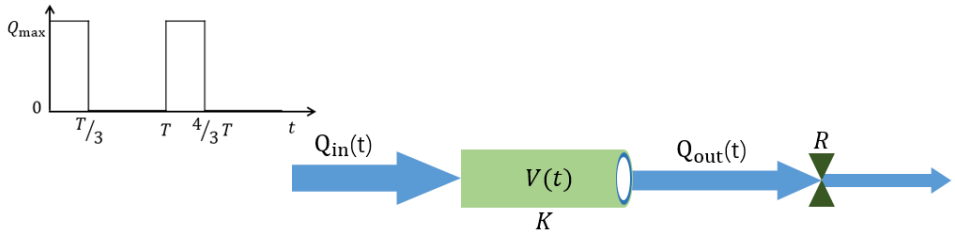

Figure 4-5 Simplified model of circulatory system

Here, volume of graft is a function of time $V(t)$, and a mass balance (assuming incompressibility of the liquid) gives

$$\frac{dV}{dt} = Q_{in}(t) - Q_{out}(t) \qquad \text{Equation 4-2}$$

The output flow rate $Q_{out}(t)$ can be written in terms of the gauge pressure (P) in the graft which drives the output flow, and the valve resistance, R, which regulates the flow. In principle, R is a function of flow rate, however here we will take it as a constant.

$$Q_{out}(t) = \frac{P}{R} \qquad \text{Equation 4-3}$$

Strictly, the numerator of the above equation should be ($P-P_{downstream}$), where $P_{downstream}$ is the pressure immediately downstream of the valve. We estimate that the downstream gauge pressure is close zero since the exit of the valve simply returns the fluid to a reservoir that is open to the atmosphere. In fact, the downstream gauge pressure is not zero since there is a few cm height differences between the valve and the reservoir. Yet, this small difference is ignored in this approximate analysis.

The gauge pressure (P) is related to the current volume of graft; specifically, the more the graft is inflated (as compared to its zero-gauge-pressure value), the higher is the expected P. We introduce a constant (K), which represents the stiffness degree of the graft. And V0 is the initial volume of graft, which can be calculated by measuring the inner diameter and the length of graft. We then adopt a simple linear relationship between volumetric inflation and the gauge pressure:

$$P = K(\mathrm{V(t)} - V_0) \qquad \text{Equation 4-4}$$

Combining equations 4-2,4-3 and 4-4,

$$\frac{dV}{dt} = Q_{in}(t) - \frac{K}{R}(V(t) - V_0) \qquad \text{Equation 4-5}$$

Where $\frac{K}{R}$ is a constant with a unit of s^{-1} and may be regarded as the rate at which an initially-inflated graft deflates when the input flow rate is set to zero. And at t = 0, equation 4-5 can be written as:

$$\frac{dV(t=0)}{dt} = Q_{in}(t=0) - \frac{K}{R}(V(t=0) - V_0) \qquad \text{Equation 4-6}$$

Subtracting equation 4-6 from equation 4-5,

$$\frac{d\bar{V}}{dt} = \overline{Q_{in}(t)} - \frac{K}{R}\overline{V(t)} \qquad \text{Equation 4-7}$$

Here, the bar notation indicates deviation variables, i.e. those that capture the deviation from the initial condition. Applying Laplace transform to this equation,

$$(\frac{R}{k}s + 1)\bar{V}(s) = \frac{R}{K}\bar{Q}(s) \qquad \text{Equation 4-8}$$

where s is a complex variable.

A MATLAB Simulink project was built on this equation 4-8 by Prof. Robert Parker (Figure 4-6).

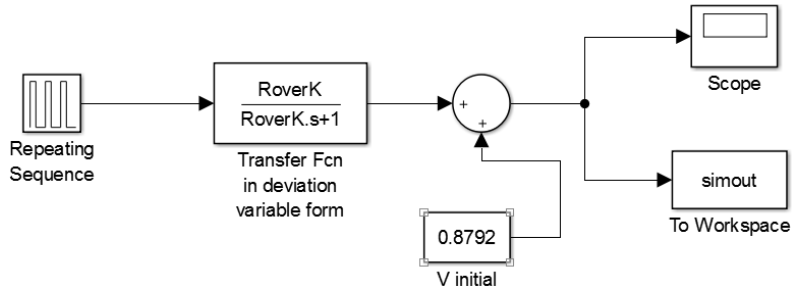

Figure 4-6 Diagram of Simulink project

In this project, input values are the initial volume of graft, input function $Q_{in}(t)$ and deflation time $\frac{R}{K}$. The output is the volume function of graft under preset conditions.

The initial volume was set to 0.8792mL, based on the estimated diameter of 4mm and length of 7cm.

We have not directly measured the deflation time. Nevertheless, since the graft visibly expands and contracts at a oscillation frequency of 100 strokes/min, deflation times must be well under 1 second. For illustration purposes, the deflation time is set to 0.1s, and frequency is set to be 20, 40, 60, 80 and 100 strokes/min. Due to different frequency, input function $Q_{in}(t)$ has

different period ($T = \frac{60}{Freq.}$) and different maximum value $Q_{max} = \frac{3V_c}{T}$, where Vc is stroke volume 6mL.

The results are plotted in Figure 4-7 and Figure 4-8 below. A higher frequency can lead to an incomplete relaxation of graft (i.e. the volume remains higher than V_0 throughout the oscillatory cycle), which is clearly shown in Figure 4-7. A higher frequency also indicates a larger volume variation, which can be considered as a larger diameter variation, over each cycle. From equation 4-4, pressure is proportional to $K(V(t) - V_0)$, which is the deviation of volume from the deflated volume. Furthermore, since R is held constant, the pressure is proportional to $\frac{K}{R}(V(t) - V_0)$. From Figure 4-8, the difference between the maximum and minimum volume can be obtained, and the quantity $\frac{K}{R}(V(t) - V_0)$ plotted against frequency, as shown in Figure 4-9. The same tendency can be found that change volume at maximum and minimum increase, indicating that high pressure and low pressure both increase with a higher frequency. This this simple model at least suggests no mechanism whereby the high and low pressures in the graft would converge.

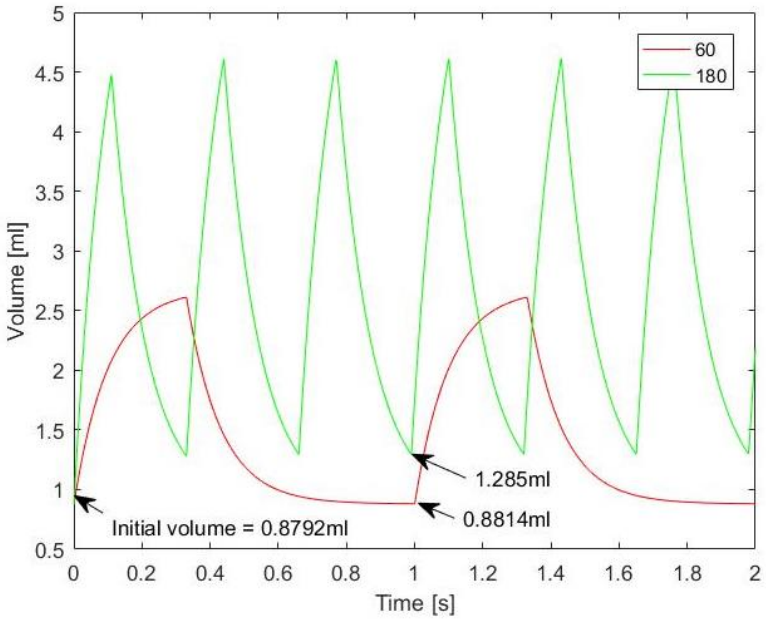

Figure 4-7 Volume function with frequency at 60 and 180 strokes/min

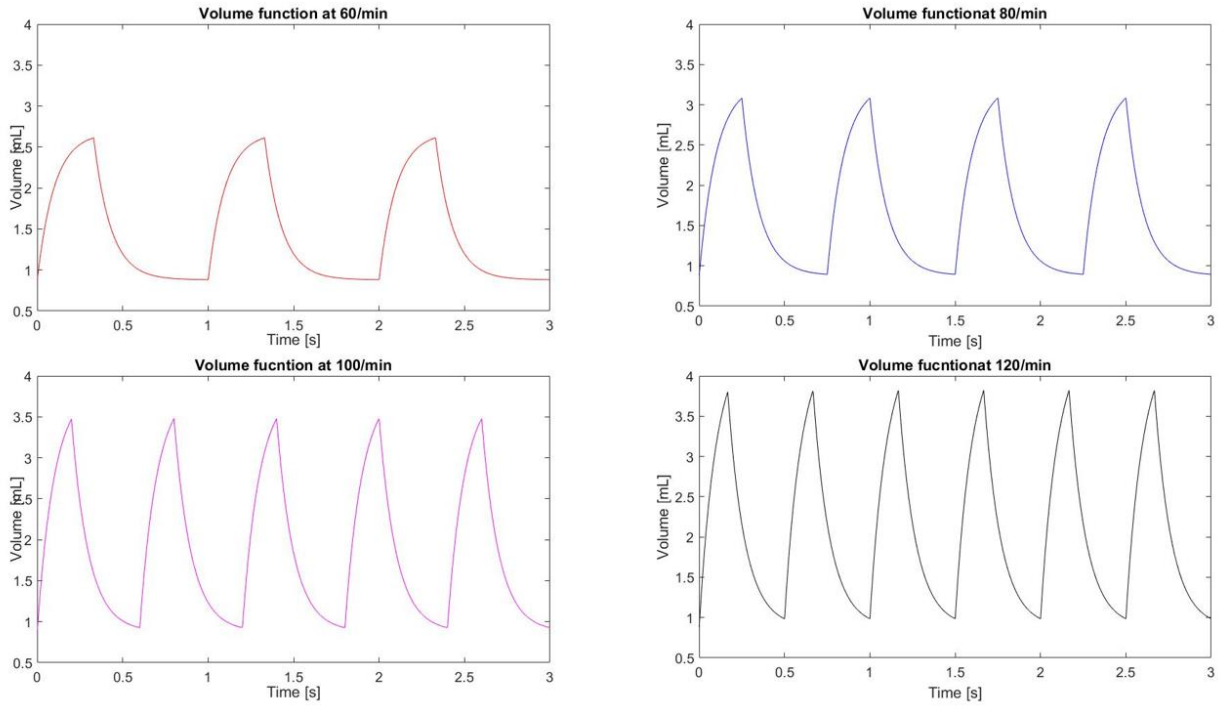

Figure 4-8 Volume function with frequency at 60, 80, 100 and 120 strokes/min

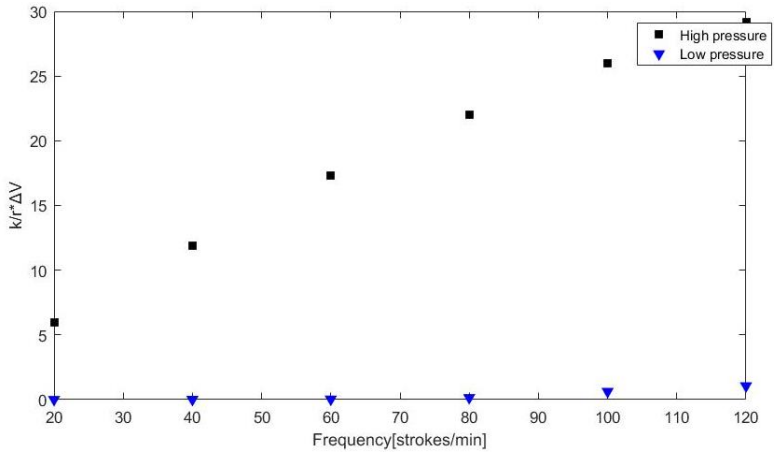

Figure 4-9 Diagram of $\frac{K}{R}(V(t)-V_0)$ vs. frequency

The ratio K/R, indicates the deflation time of the graft. Under the frequency of 80 strokes/min, $R/_k$ is assigned to be 0.033, 0.1 and 0.3 seconds. Figure 4-10 plots the volume vs. time for these conditions. For each condition, the quantity $\frac{K}{R}(V(t)-V_0)$ plotted against frequency is shown in Figure 4-11. And it can be found that that ratio of K and R does not change the result qualitatively, but grafts that deflate rapidly reach the fully-relaxed volume during the deflation phase of the cycle.

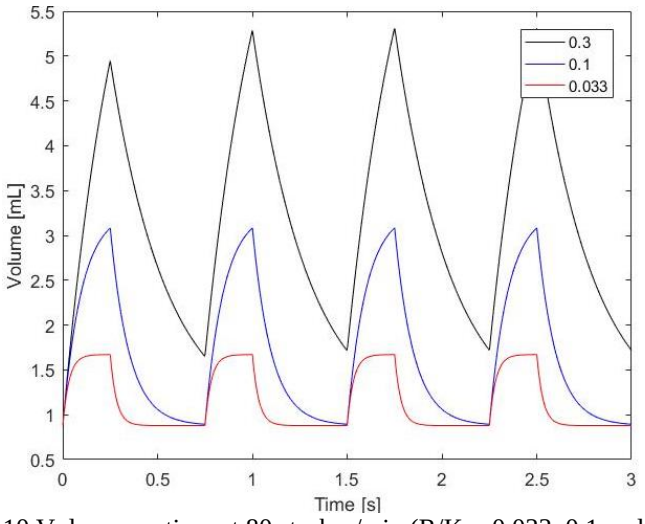

Figure 4-10 Volume vs. time at 80 strokes/min (R/K = 0.033, 0.1 and 0.3s)

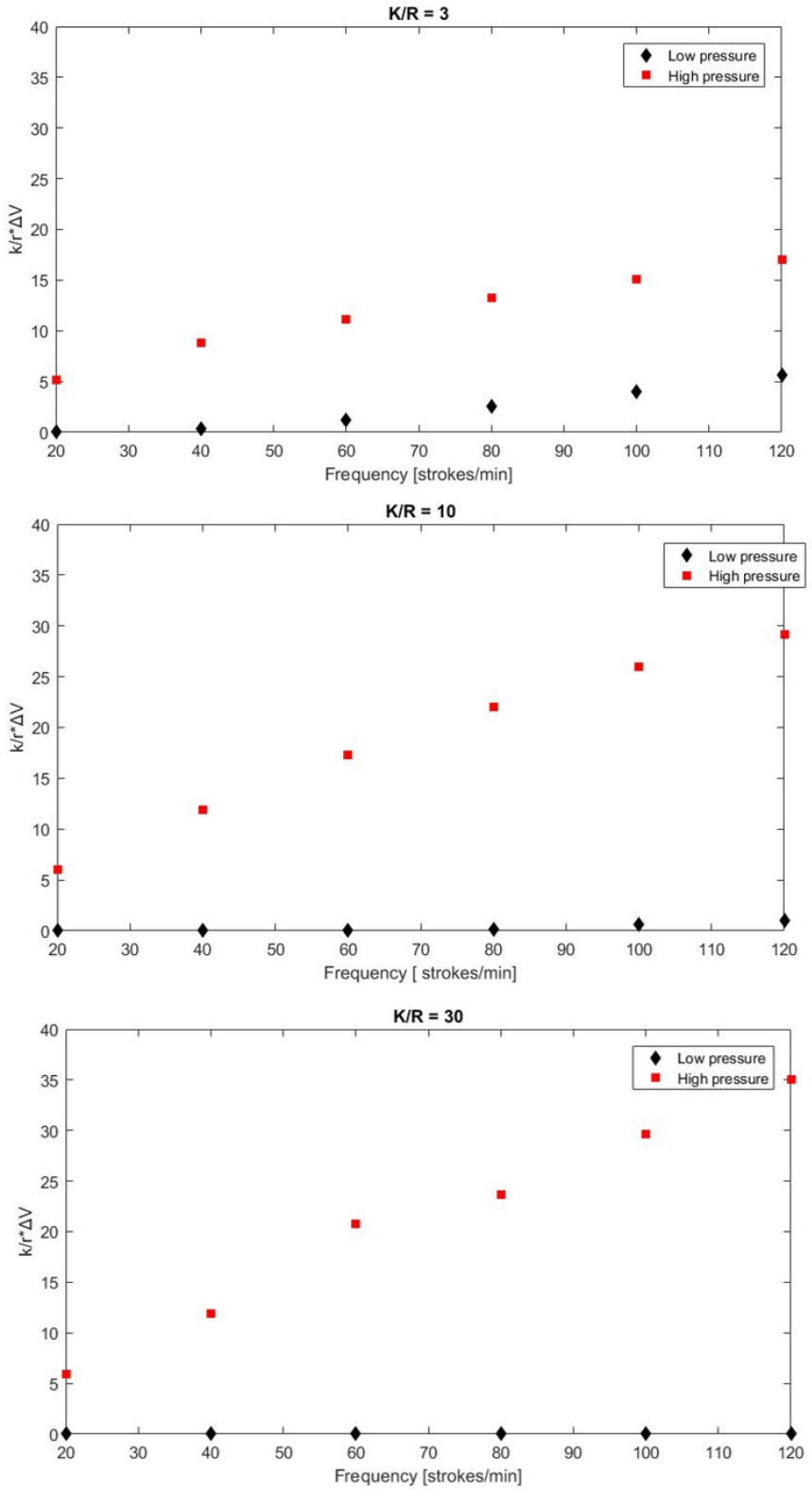

Figure 4-11 Diagram of $\frac{K}{R}(V(t)-V_0)$ vs. frequency

Several comments are needed regarding the assumptions of the model. This 1-dimensional model assumes the flow can be regarded as quasi-static. Strictly speaking, inertial effects due to the pulsatile motion may also play a role. This can be judged by evaluating the, Womersley number, Wo,[33]

$$Wo = \frac{L}{2}\sqrt{\frac{n}{\nu}} \qquad \text{Equation 4-9}$$

Where L is radius of this graft/tube, n is the frequency in radius, and ν is the kinematic viscosity of the fluid, which is water here. Substituting the diameter 2mm, frequency $2\pi\times\frac{freq.}{60}$ and kinematic viscosity of water $1\times10^{-6}\ m^2/s$, and Womersley number is 2.89 when frequency is 80 strokes per minute. Thus, this flow cannot be regard as strictly "quasi-steady".

We have also assumed that graft is the only compliant element in the circuit and the volume changes of the tubing is negligible. Using the diameter of tygon tube of 6.35 mm and length at 40 cm, volume of tube can be calculated, which is around 12.7 cm^2. Visually at least, the compliant tubing does not undergo significant changes in dimension. Even if we assume that the tubing undergoes up to 1% change in volume under the pulsatile flow conditions, this corresponds to 0.12 mL of the volume change. The grafts undergo diameter changes on the order of 10% or more, and hence volume changes on the order of 20%, which corresponds to roughly 0.17 mL. Thus, even small percentage volume changes of the tubing may give rise to volume fluctuations that are comparable to the graft fluctuations. Thus, the assumption that the entire compliance of the flow circuit is in the tubing must be verified by directly measuring the compliance of the

tubing. Finally, we have assumed that the main resistance to flow is the valve. To get the friction resistance, Reynold number, *Re*, indicating the flow pattern, needs to be given.[34]

$$Re = \frac{\rho v_0 L_0}{\eta} \qquad \text{Equation 4-10}$$

Where, v_0 is a characteristic velocity, and L_0 is a characteristic length. ρ is the density of the fluid and η is its dynamic viscosity. Equation 4-10 can also be written as,

$$Re = \frac{4Q}{\pi D \nu} \qquad \text{Equation 4-11}$$

By substituting the flow rate of fluid Q, which is 24mL/s for maximum under 80 strokes/min; kinematic viscosity, ν, (the ratio of the dynamic viscosity to the density of the fluid), which for water at 25℃ is $1.00356\times10^{-6}\ m^2/s$); and the diameter of the tube D (6.35mm). Reynolds number is 4798 for this condition. Through Blasius formula [34], [35], friction factor can be estimated,

$$f = \frac{0.0791}{Re^{0.25}} \qquad \text{Equation 4-12}$$

f is 9.5×10^{-3} for the tygon tube. Hence the pressure gradient can be calculated as, [34]

$$\frac{p_0 - p_L}{L} = \left(\frac{4}{D}\right)\left(\frac{1}{2}\rho v^2\right) f = \frac{2}{D}\rho\left(\frac{4\varpi}{\pi D^2 \rho}\right)^2 f = \frac{32\varpi^2 f}{\pi^2 D^5 \rho} \qquad \text{Equation 4-13}$$

Here, ϖ is the mass rate, which is 8 g/s for the average of this fluid. The result from equation 4-13, is $0.01425\ mmHg/cm$. For tube with a length of 40 cm, the total pressure drop is 0.57 mmHg which is a small fraction of the total pressure drop which is several tens of mm of Hg.

As to the local resistance from the valve, the fluid flow experiences a change in cross-section area, which is 31.65 mm2 for the tubing to less than 7 mm^2 for the valve. It can be simplified to a model that fluid flow through a thin orifice, shown in Figure 4-12. From handbook, discharge coefficient (Cd) for this orifice is 0.6.[36]–[38]

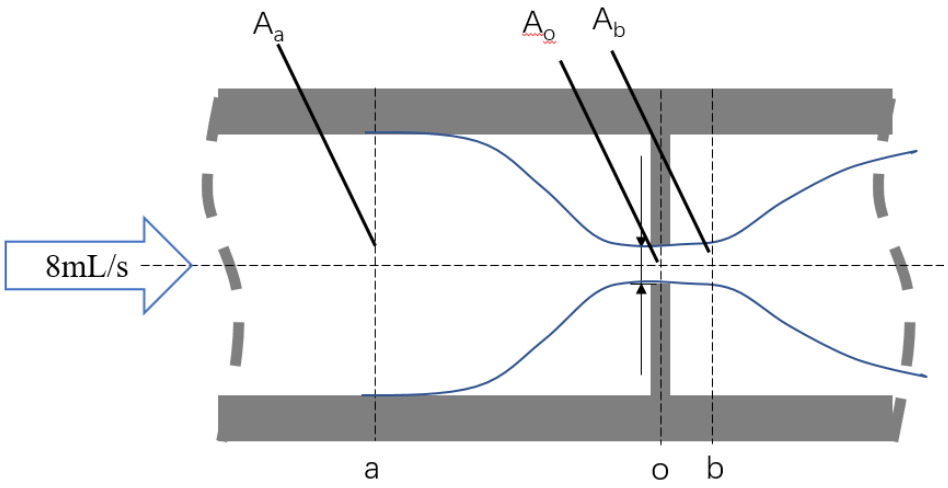

Figure 4-12 Flow through orifice

By applying Bernoulli's equation to cross section a (orifice upstream) and cross-section b (orifice downstream), should obtain,

$$P_a + \frac{1}{2}\rho v_a^2 = P_b + \frac{1}{2}\rho v_b^2 \qquad \text{Equation 4-14}$$

P is the static pressure, v is the average velocity at this two section. Since inlet and out let flow rate are the same, which is, $Q = A_a \cdot v_a = A_b \cdot v_b$. Furthermore, the area of section "o" and section "b" is much smaller than inlet area "a", so the velocity in section "a" (v_a) is neglected.

Simplifying equation 4-14, one get [39]–[42]

$$P_a - P_b = \frac{\rho}{2}\left(\frac{Q}{C_d \times A_o}\right) \qquad \text{Equation 4-15}$$

Subsisting the density of water at 25℃, which is 1000kg/m^3; Average flow rate, 8 mL/s; C_d is 0.6, A_o is 7 mm^2, the pressure drop through this orifice is 1814 Pa, which is 13 mmHg. By comparing the friction resistance from the tube and local resistance from the valve, one can conclude that the resistance for the tube can be neglected. Thus, the assumption that the main resistance to flow is from the valve appears to be justified.

5.0 VALIDATION EXPERIMENT

Although the idea that changes in surface topography could eliminate clots driven by pressure drop was authenticated by previous experiments by Dr. Pocivavsek, the graft developed in this project has not yet been validated to reduce blood fouling. To test whether the graft could function well and decrease biofouling deposition, a liquid which can show bio-fouling is needed. Here, bovine whole blood and expired platelet-rich plasma (PRP) is used. PRP is plasma with 3-8 times the concentration of normal platelet levels (150,000 to 400,000 platelets per microliter), and contains almost none of other kind of blood cells. The concentration of platelets and growth factors can be 5 to 10 times greater (or richer) than usual.[43], [44] Platelets are very important to blood clotting. The activation of platelets can trigger the activation of more than 30 substances, most of them are proteins. Together they build up clots and prevent blood loss from wounds.[45], [46] Although the PRP used here is expired, platelets still have a sufficient activity that they can adhere, aggregate and build clots. However, it could take hours, even days for platelets clotting by themselves. To accelerate this process, a small amount of thrombin (from human plasma) is added to the PRP before the start of the experiment. Detailed information of materials and solutions are listed in Table 5-1. The effect of thrombin is shown in Figure 5-1, one dish contains only PRP (25 ml), and the other one has the same amount of PRP, but with 30μL of thrombin stock solution, which contains 3 units of thrombin. After two hours at room temperature, there are obvious flocs in the PRP with thrombin, and no significant change to

thrombin-free PRP added. We presume that these flocs formed by activated platelets and other proteins. Due to the high-activity of thrombin, quantity of it need to be controlled. Too much of thrombin will lead to a high viscosity of liquid and also blockage in the system, which will damage the pump. However, less thrombin may take a long time for clot formation, and clots adhere to luminal surface might be less, which could impact the result. To Figure the necessary quantity of thrombin, various amount (3, 5, 10 and 20 units) of thrombin were added into 25mL of PRP, coagulation time is recorded. Under room temperature, expired PRP with 10 and 20 units formed a gel-like block within 1 minute. For those with 3 and 5 units, it took over 50 mins and 10mins respectively.

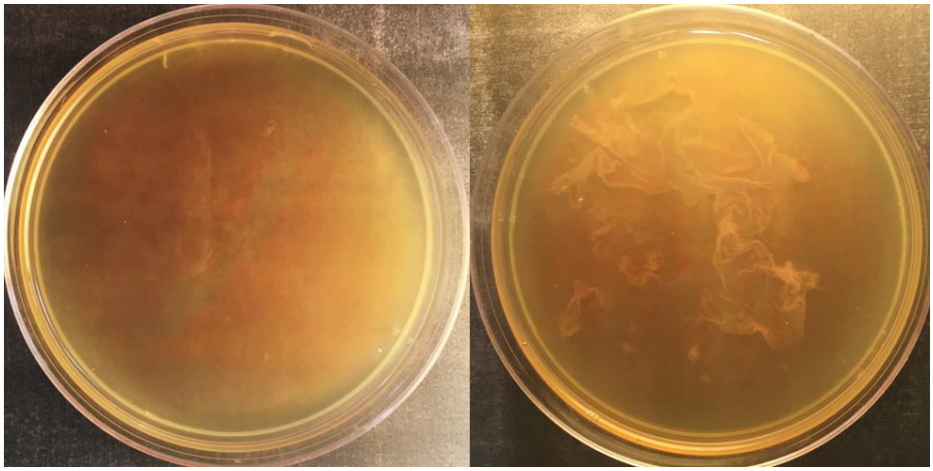

Figure 5-1 Comparision of 25 mL expired PRP with none (left) and 3 units (right) of thrombin after 2h at room temperature

To test that actuation of the grafts reduces clot adhesion, a control sample (which does not pulsate) is needed. This control sample is made by coating several GI-380 stiffening layers on the outside of the cylinder, and then further immobilized by adhesive tape. However, the control has the similar luminal surface wrinkled topography as the test sample. In this case, it will remain rigid during the pulsatile flow experiment.

Table 5-1 Detailed information of materials and solutions

Name	Concentration	Amount (per experiment)	Vendor	Notes
Thrombin stock solution	100 units/ml in 0.1% (w/v) BSA solution	300 μL	EMD Millipore	For PRP experiment
Thrombin stock solution	100 units/ml in 0.1% (w/v) BSA solution	400 μL	EMD Millipore	For whole blood experiment
Bovine Whole blood in Sodium Heparin	N/A	~250mL	Lampire Biological Laboratories	Consumed 13 after bleed date
Expired PRP	150,000 to 400,000 platelets /mL	~250mL	Central Blood Bank	Consumed within a week after expire date
Wright stain solution	N/A	~10mL	Fisherbrand	Dark Purple
4% Buffered Formalin solution	40g of paraformaldehyde in 1L 1X PBS solution	~100mL	PROTOCOL	
PBS without Calcium or Magnesium	1X PBS solution	~50mL	Lonza	

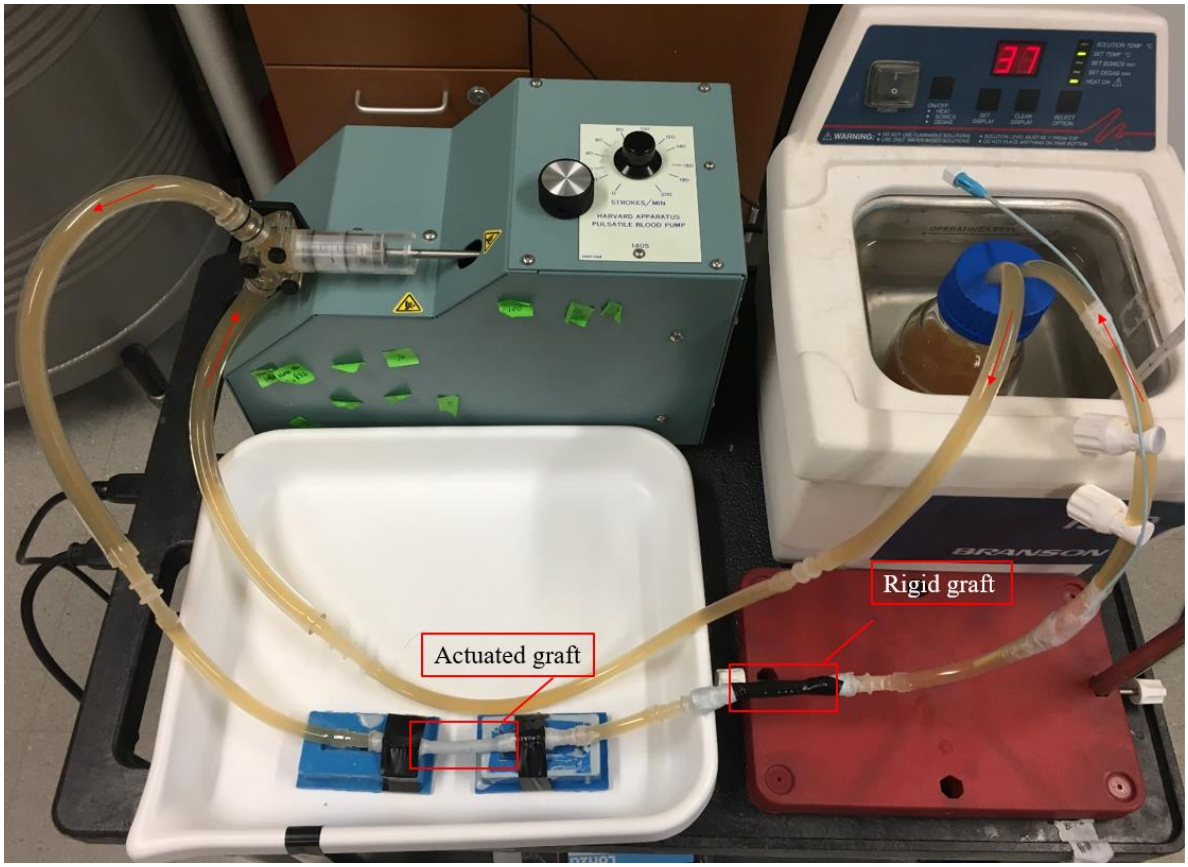

Figure 5-2 Circulatory system run with expired PRP

The two samples were connected by a Tygon tube in series, and expired PRP (3 bags, about 250ml) with 300μL thrombin stock solution (corresponding to 30 units of thrombin) added was held in a 250ml - glass media bottle, immersed in a water bath at 37C.

The pulsatile flow experiment was run at rate of 80 stokes/minute over 4hours. At the end of the experiment, the two grafts were cut off from this circulatory system. They were rinsed with Phosphate Buffered Saline (PBS) solution gently to remove the extra clots not attaching to the surface. After rinsing 3~5 times, the samples were soaked in 4% Buffered Formalin solution to complete the fixation of protein and cells (thrombus patch) for 24 hours at room temperature. For following staining process, fixation is very important, since it could stabilize the clots and protect samples against microbial contamination and decomposition, thus permitting ex-situ

imaging. To get a better view of the inside, grafts were cut from the middle. For staining the clot, two grafts were bisected in half along their axis creating two equal hemicylinders, which allow the inside surface to have a better contact with Wright-Giemsa stain. Wright-Giemsa stain is commonly used for blood smears, usually blood cells present a color of purple.[47] The actual procedure for used staining with Wright-Giemsa stain has been listed in the Appendix B. Clots color in dark purple after stain. As shown in Figure 19, the difference of the fouling situation between two grafts is apparent to even to naked eyes. There is a large clot forming in the static graft (Figure 5-3), which even blocked the whole flow circuit; So, the controlled sampled had to be removed 30 mins earlier than planned. As to the actuated graft, there is much less clot forming in it. With a closer look for these two grafts (Figure 5-4), further significant difference could be identified: the actuated sample maintained a relative clean surface with much less platelet deposition on its surface. By contrast, more clots attached to the inner surface of static sample, which was heavily contaminated within four hours. Same experiments were conducted for 4 times and similar result is achieved.

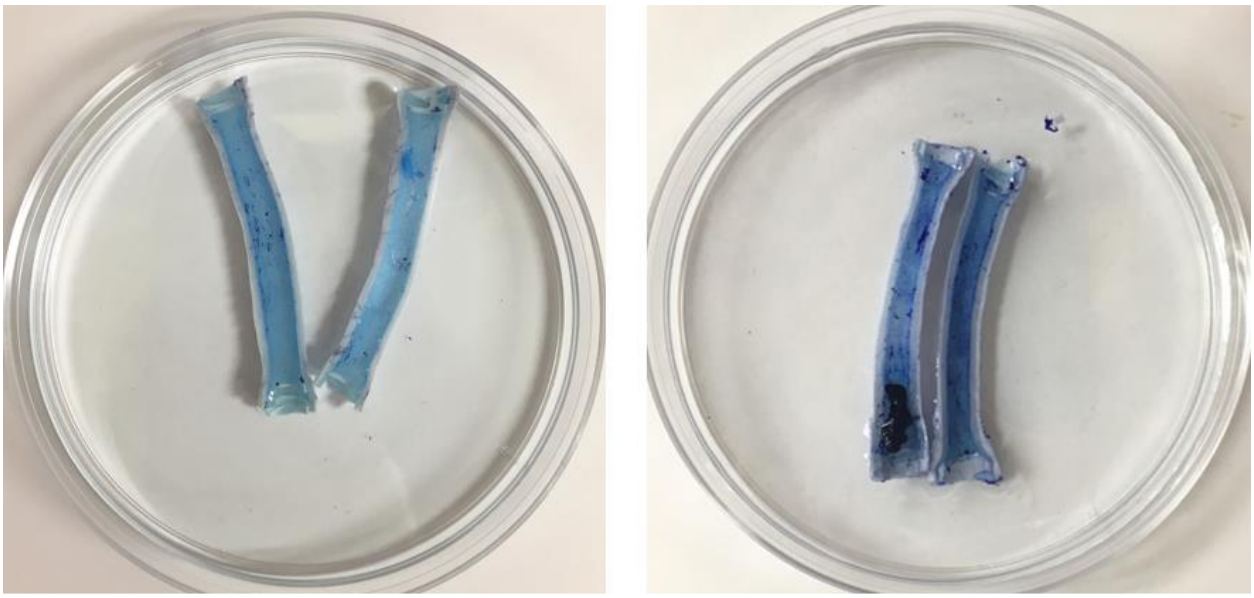

Figure 5-3 Luminal surface of actuated graft (left) and static graft (right) with PRP

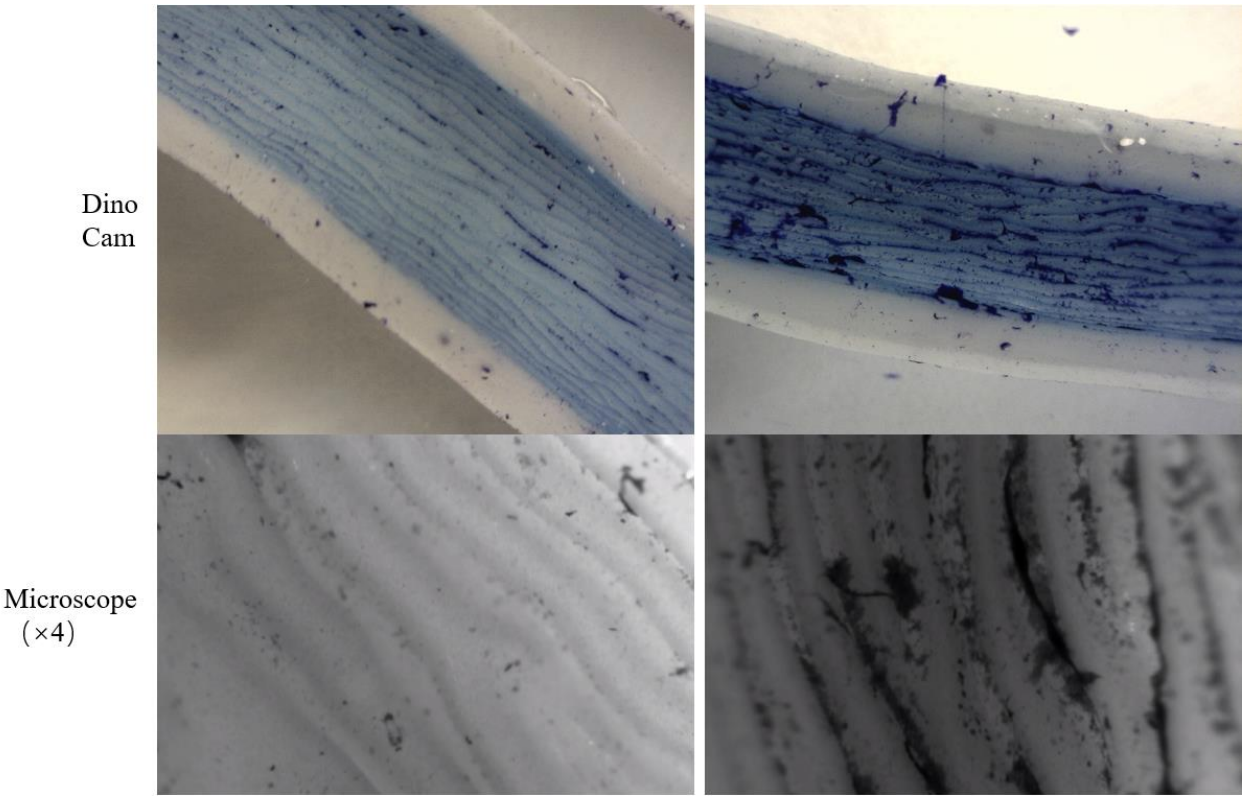

Figure 5-4 Luminal surface of actuated graft (left column) and static graft (right column) with PRP

Besides running with PRP, whole blood (see table 5-1 for details) is also introduced to this process. Two samples were run by bovine whole blood (250mL) and 400μL of thrombin stock solution (40 units of thrombin). Since anticoagulant was added to whole blood, the amount of thrombin was necessary to complete the experiment in a reasonable time. The viscosity of whole blood is 3-5 times than the viscosity of PRP[48], and it is much more rich in blood cells and proteins. The clot forming speed was much higher than PRP, and so the viscosity increases as well. Due to these two factors, this experiment was only run for 1.5 hours. The remaining experimental conditions remained the same as for the PRP experiment. The results are shown in Figure 5-5 and 5-6. Even with the shorter time, the difference between actuated and static grafts remain.

Thus, is clearly that luminal surface remains cleaner when it is actuated, which indicates that grafts could function well with PRP and whole blood under expected pressure.

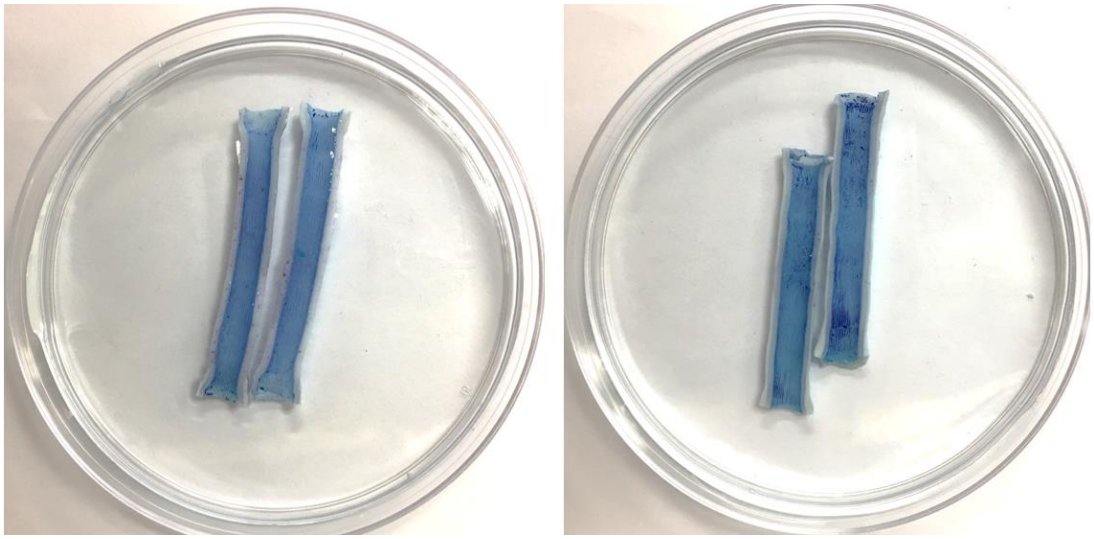

Figure 5-5 Luminal surface of actuated graft (left) and static graft (right) with Bovine whole blood

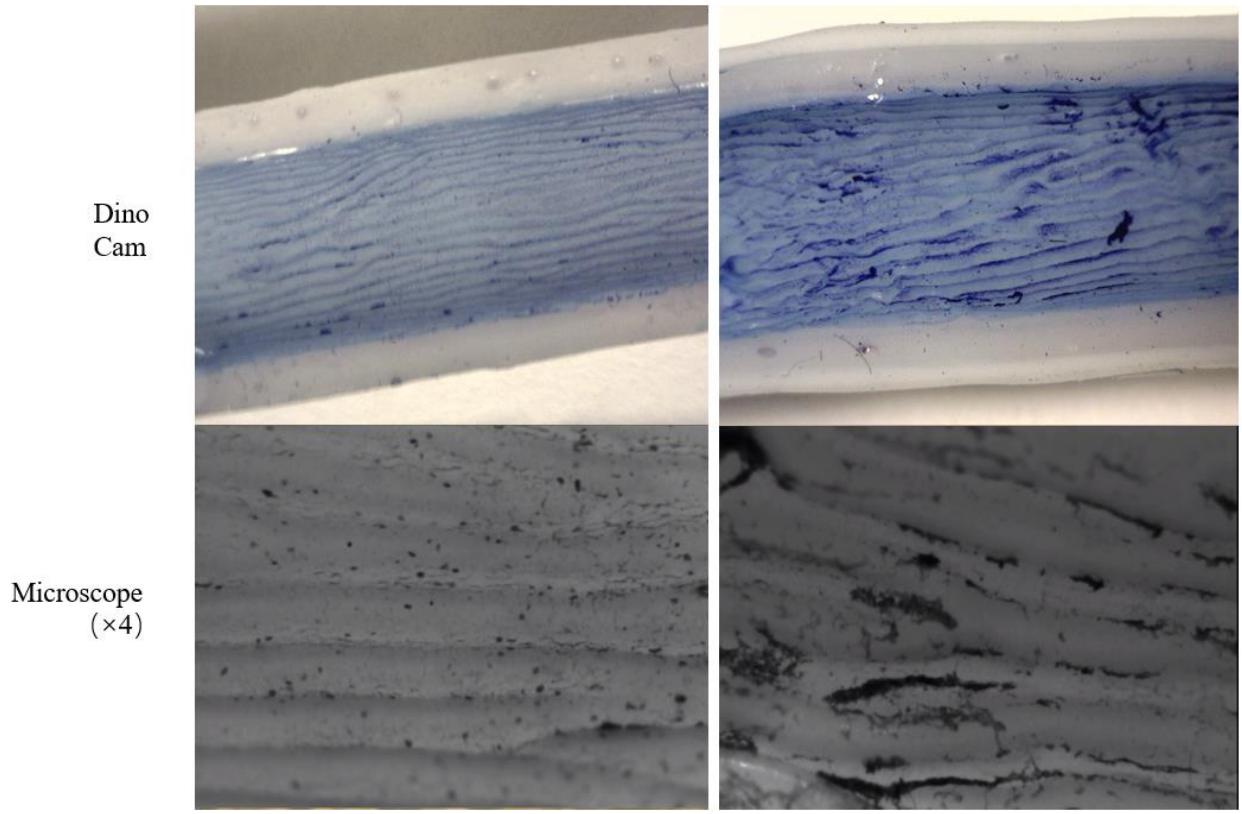

Figure 5-6 Luminal surface of actuated graft (left column) and static graft (right column) with bovine whole blood

6.0 SUMMARY AND PERSPECTIVES

From what has been discussed above, this featured graft with small diameter (<6mm) function well under desired pressure range. Following animal experiments also proved that its luminal surface is qualified as self-clean when actuated. However, there are still lots questions needed to be solved.

The first problem countered is the huge mismatch between calculation and measurement. Reasons for this discord may be the mismeasurement of moduli, or materials show different physical properties when they are prepared differently. And there are expiration dates for each of these silicone-based polymer, they might deteriorate after some time, also still within the recommended date. This deterioration may lead to an increasing or a decreasing in stiffness of polymers.

Second problem is the phenomenon that low pressure and high pressure appear to overlap with each other at 100 per minute. One possible reason guess for this is that this is an artifact of the display frequency of sensor panel being close to consistent with the pattern of pressure change, in this case, pressure appears to keep at the almost the same values. A higher frequency pressure measurement could be applied for further study to fix this problem.

Third is the assumption that the volume changes of the tubing are negligible. However, through calculations it is found that a small percentage volume changes of the tubing may give rise to volume fluctuations that are comparable to the graft fluctuations. In this case, the

assumption that the entire compliance of the flow circuit is in the tubing must be verified by directly measuring the compliance of the tubing. Or these tygon tubes could be replaced by other kind of tubes, which are more rigid, like metal tubes.

There are also some improvements. As discussed in chapter 2.2, another than actuated wrinkled sample, the actuated flat sample also shows a good performance in reducing bio-fouling. However, in validation experiment, actuated flat graft is not tested. For the integrity for this research, actuated flat sample needs to be tested as well. Then, the graft length needs to be increased for practical applications. Current graft length is about 7 cm in average (Figure 3-5a). For surgeries, the optimal length is over 10cm. However, it is limited by current construction strategy, especially by the tools used. Thus, fabrication method should be improved in order to increase graft length. Indeed ideally, it would be desirable to manufacture continuous graft tubing that can be cut to the desired lengthy the surgeon. The instrument used as dip coater could be transformed, in order to provide more vertical work space. Although initial success is obtained, this graft has never been tested over 5 hours. Long-term experiments, counted by days, should be applied, to find out its durability and performance in a relatively long time.

Previously Dr. Pocivavsek studied the influence of the size of wavelength in chapter 2.3, and found that a smaller wavelength could give less platelet deposition. However, we have not studied wavelength effects our blood or PRP experiments. When the wavelength is small enough (e.g. sub-micron), we may expect the luminal surface could be “effectively” flat, i.e. the platelets or the platelet clots would no longer be able to “see” the change from smooth to rough. In this case, we anticipate graft will not reduce bio-fouling. To know the right range of wavelength, fabrication method need to be improved, and grafts with small wavelength, much less than 80 microns, should be studied.

For the future study, current materials are enough for carry in vitro experiments and tests. However, when it comes to in vivo experiments or surgeries, it needs to be replaced by other material which is easier for human bodies to tolerate, and maintain its feature for long-term, and FDA approved.

APPENDIX A

DIAGRAM OF STRESS-STRAIN

Following data was collected by Mr. Joseph Pugar. Polymers were constructed into a dog bone-shape batch, then tested with standard multicycle tensile test.

Graph of stress-strain of all polymers were shown below.

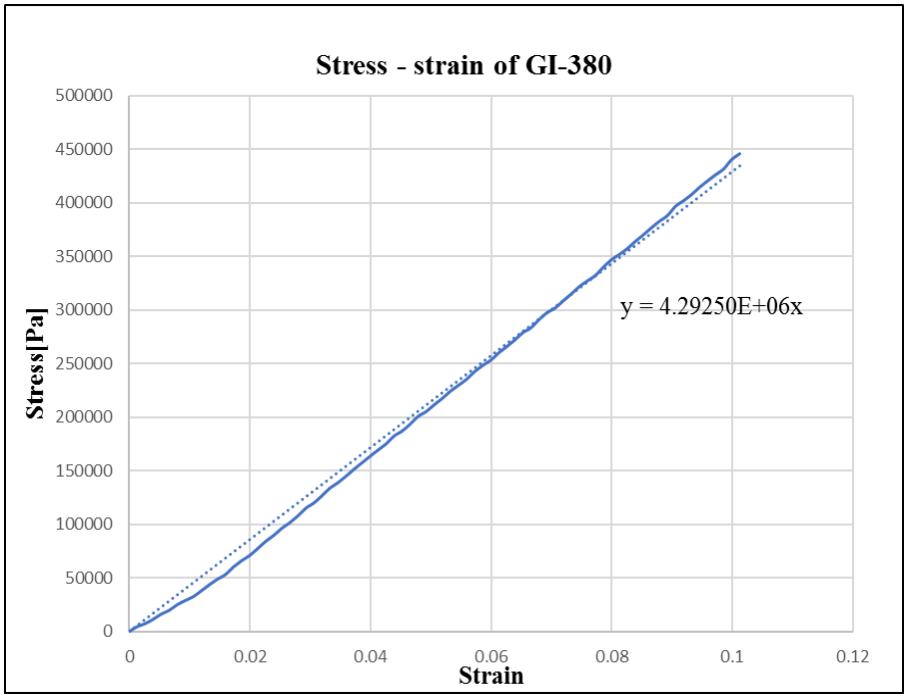

Figure A.1 Stress-strain of GI-380 with 10%(w/w) crosslinker added

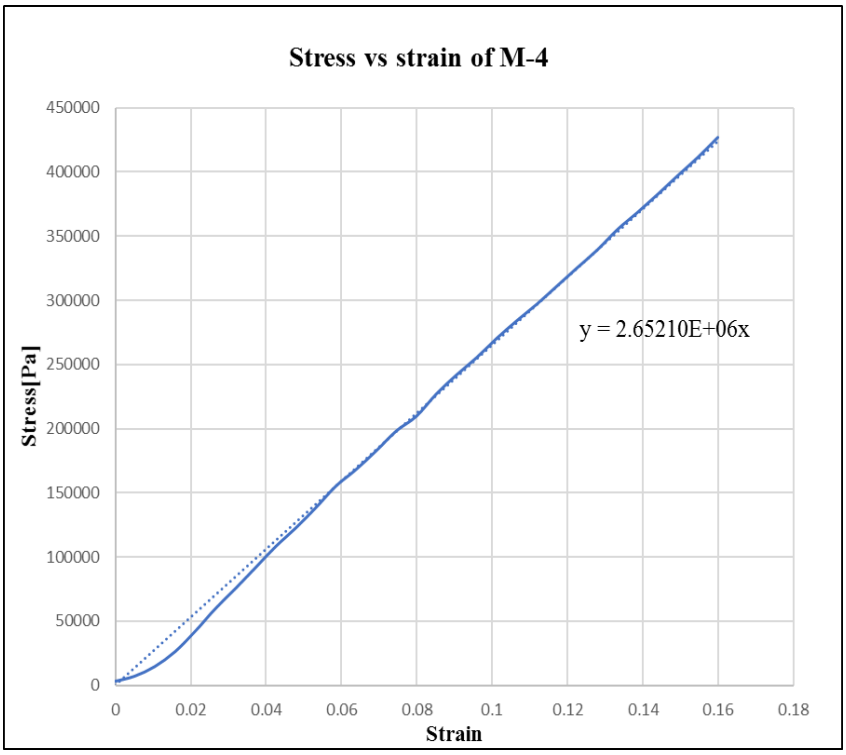

Figure A.2 Stress-strain of M-4 with 10%(w/w) crosslinker added

Figure A.1 and A.2 are diagram of GI-380 and M-4, when 10% (w/w) of crosslinker is added. After applying with a linear fitting, two linear function could be calculated. And slopes of these two function are the moduli of GI-380 and M-4 respectively.

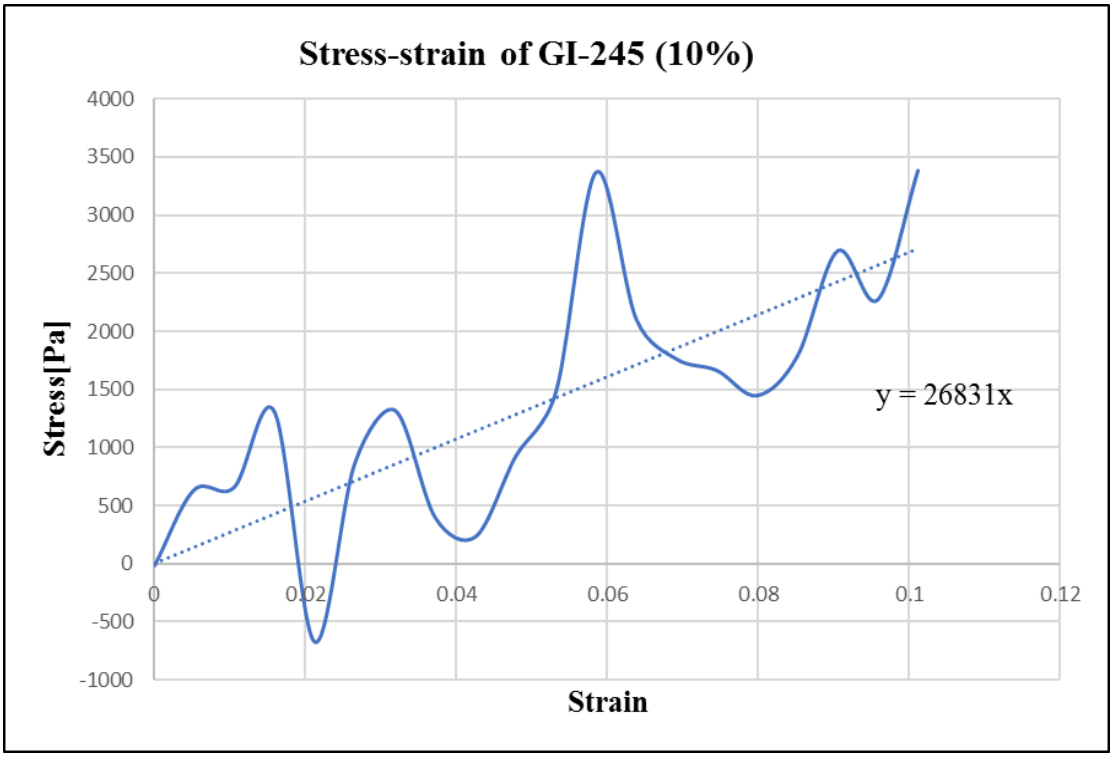

Figure A.3 Stress-strain of GI-245 with 10%(w/w) crosslinker added

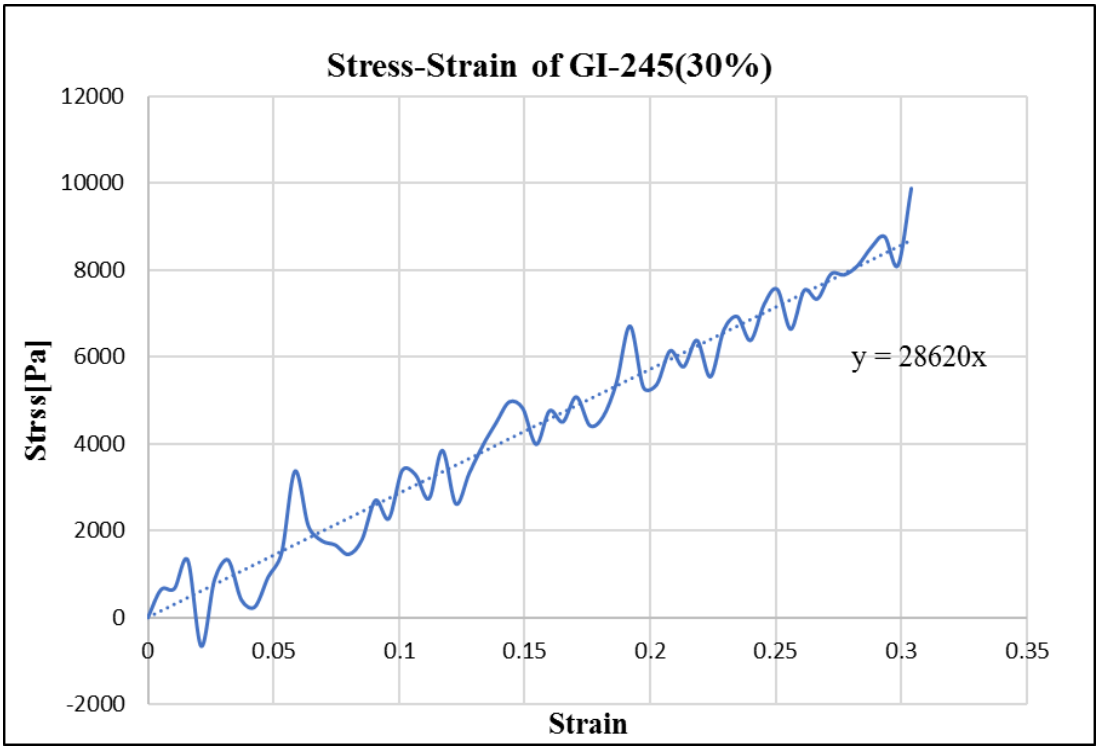

Figure A.4 Stress-strain of GI-245 with 30%(w/w) crosslinker added

In Chapter 3, 20% of crosslinker is added to GI-245 to construct substrate. However, moduli of GI-245 with 10% and 30% crosslinker is tested, which are 26831 and 28620 Pa respectively. In this case, modulus of GI-245 with 20% of crosslinker is decided to be intermediate value of these two numbers, which is 27.7 kPa.

APPENDIX B

STAIN PROCEDURE

1. Take one buffer tablet. Dissolve it with 1000 mL deionized water.

2. Put the bisected graft into a glass petri dish, with a diameter of 10 cm. Fixing the graft with Methyl Alcohol for 60 seconds. Remove the excess methanol from the dish.

3. Cover the graft with 3 mL of Wright-Giemsa stain and allow to stain for 2 minutes.

4. Add 4.5 mL of PH 6.4 Diluted Buffer to the stain-covered graft.

5. By rocking the dish genteelly to mix the stain and buffer solution together about 1 minute. Leave the mixture to stain the graft for an additional 3 minutes.

6. Rinse the graft with PBS solution and allow it to air dry.

BIBLIOGRAPHY

[1] A. T. Hirsch *et al.*, "A Call to Action: Women and Peripheral Artery Disease," *Circulation*, vol. 125, no. 11, p. 1449 LP-1472, Mar. 2012.

[2] A. Perez Perez *et al.*, "Obesity and cardiovascular disease," *Public Health Nutr.*, vol. 10, no. 10 A, pp. 1156–1163, 2007.

[3] S. Mendis, P. Puska, and B. Norrving, "Global atlas on cardiovascular disease prevention and control," *World Heal. Organ.*, pp. 2–14, 2011.

[4] "WHO | Cardiovascular diseases (CVDs)," *WHO*, 2016.

[5] R. H. HELFANT, J. S. FORRESTER, J. R. HAMPTON, J. I. HAFT, H. G. KEMP, and R. GORLIN, "Coronary Heart Disease," *Circulation*, vol. 42, no. 4, p. 601 LP-610, Oct. 1970.

[6] "What Is Coronary Heart Disease? - NHLBI, NIH," *National Institutes of Health; Department of Health and Human Services;USA.gov*, 2016. [Online]. Available: https://www.nhlbi.nih.gov/health/health-topics/topics/cad. [Accessed: 07-Mar-2017].

[7] "What Is Peripheral Artery Disease? - NHLBI, NIH," *National Institutes of Health;Department of Health and Human Services;USA.gov*, 2016. [Online]. Available: https://www.nhlbi.nih.gov/health/health-topics/topics/pad. [Accessed: 07-Mar-2017].

[8] K. Ouriel, "Peripheral arterial disease," *Lancet*, vol. 358, 2001.

[9] "How Is Coronary Heart Disease Treated? - NHLBI, NIH," *National Institutes of Health, Department of Health and Human Services, USA.gov*, 2016. [Online]. Available: https://www.nhlbi.nih.gov/health/health-topics/topics/cad/treatment#MedicalProceduresSurgery. [Accessed: 08-Mar-2017].

[10] "How Is Peripheral Artery Disease Treated? - NHLBI, NIH," *National Institutes of Health, Department of Health and Human Services, USA.gov*, 2016. [Online]. Available: https://www.nhlbi.nih.gov/health/health-topics/topics/pad/treatment. [Accessed: 08-Mar-2017].

[11] S. P. Saha, T. F. Whayne, and J. and D. Mukherjee, “Current Evidence for Antithrombotic Therapy after Peripheral Vascular Interventions,” *Current Vascular Pharmacology*, vol. 11, no. 4. pp. 507–513, 2013.

[12] JEAN E. STARR, “Surgical Bypass,” *Society for Vascular Surgery*, 2004. [Online]. Available: https://vascular.org/patient-resources/vascular-treatments/surgical-bypass. [Accessed: 08-Mar-2017].

[13] G. Punshon, K. M. Sales, D. S. Vara, G. Hamilton, and A. M. Seifalian, “Assessment of the potential of progenitor stem cells extracted from human peripheral blood for seeding a novel vascular graft material,” *Cell Prolif.*, vol. 41, no. 2, pp. 321–335, Apr. 2008.

[14] P. L. Faries *et al.*, “A comparative study of alternative conduits for lower extremity revascularization: All-autogenous conduit versus prosthetic grafts,” *J. Vasc. Surg.*, vol. 32, no. 6, pp. 1080–1090, Dec. 2000.

[15] P. Klinkert, P. N. Post, P. J. Breslau, and J. H. van Bockel, “Saphenous vein versus PTFE for above-knee femoropopliteal bypass. A review of the literature,” *Eur J Vasc Endovasc Surg*, vol. 27, 2004.

[16] R. D. Sayers, S. Raptis, M. Berce, and J. H. Miller, “Long-term results of femorotibial bypass with vein or polytetrafluoroethylene,” *Br J Surg*, vol. 85, 1998.

[17] C. P. Twine and A. D. McLain, “Graft type for femoro-popliteal bypass surgery,” in *Cochrane Database of Systematic Reviews*, no. 5, C. P. Twine, Ed. Chichester, UK: John Wiley & Sons, Ltd, 2010, p. CD001487.

[18] R. Y. Kannan, H. J. Salacinski, P. E. Butler, G. Hamilton, and A. M. Seifalian, “Current status of prosthetic bypass grafts: A review,” *J. Biomed. Mater. Res. Part B Appl. Biomater.*, vol. 74B, no. 1, pp. 570–581, Jul. 2005.

[19] J. D. Kakisis, C. D. Liapis, C. Breuer, and B. E. Sumpio, “Artificial blood vessel: The Holy Grail of peripheral vascular surgery,” *J. Vasc. Surg.*, vol. 41, no. 2, pp. 349–354, Mar. 2005.

[20] M. R. Hoenig, G. R. Campbell, B. E. Rolfe, and J. H. Campbell, “Tissue-Engineered Blood Vessels,” *Arterioscler. Thromb. Vasc. Biol.*, vol. 25, no. 6, p. 1128 LP-1134, May 2005.

[21] M. Tatterton, S.-P. Wilshaw, E. Ingham, and S. Homer-Vanniasinkam, “The Use of Antithrombotic Therapies in Reducing Synthetic Small-Diameter Vascular Graft Thrombosis,” *Vasc. Endovascular Surg.*, vol. 46, no. 3, pp. 212–222, Feb. 2012.

[22] N. R. Tai, H. J. Salacinski, A. Edwards, G. Hamilton, and A. M. Seifalian, “Compliance properties of conduits used in vascular reconstruction,” *Br. J. Surg.*, vol. 87, no. 11, pp. 1516–1524, Nov. 2000.

[23] H. J. Salacinski *et al.*, “The Mechanical Behavior of Vascular Grafts: A Review,” *J. Biomater. Appl.*, vol. 15, no. 3, pp. 241–278, Jan. 2001.

[24] K. Berger, L. R. Sauvage, A. M. Rao, and S. J. Wood, “Healing of arterial prostheses in man: its incompleteness.,” *Ann. Surg.*, vol. 175, no. 1, pp. 118–127, Jan. 1972.

[25] S. Sarkar, K. M. Sales, G. Hamilton, and A. M. Seifalian, “Addressing thrombogenicity in vascular graft construction,” *J. Biomed. Mater. Res. Part B Appl. Biomater.*, vol. 82B, no. 1, pp. 100–108, Jul. 2007.

[26] G. H. Engbers and J. Feijen, “Current techniques to improve the blood compatibility of biomaterial surfaces.,” *Int. J. Artif. Organs*, vol. 14, no. 4, pp. 199–215, Apr. 1991.

[27] J. E. Greensmith and B. R. Duling, “Morphology of the constricted arteriolar wall: physiological implications.,” *Am. J. Physiol.*, vol. 247, no. 5 Pt 2, pp. H687-98, Nov. 1984.

[28] Z. Y. Huang, W. Hong, and Z. Ã. Suo, “Nonlinear analyses of wrinkles in a film bonded to a compliant substrate,” vol. 53, pp. 2101–2118, 2005.

[29] B. S. Yang, K. Khare, and P. Lin, “Harnessing Surface Wrinkle Patterns in Soft Matter,” vol. 10617, no. 1, pp. 2550–2564, 2010.

[30] C. M. Stafford *et al.*, “A buckling-based metrology for measuring the elastic moduli of polymeric thin films,” *Nat Mater*, vol. 3, no. 8, pp. 545–550, Aug. 2004.

[31] S. Y. Pei-Chun Lin, “Spontaneous formation of one-dimensional ripples in transit to highly ordered two-dimensional herringbone structures through sequential and unequal biaxial mechanical stretching,” *Appl. Phys. Lett.*, vol. 90, no. 24, p. 241903, Jun. 2007.

[32] J. F. Arevalo, Ed., *Retinal Angiography and Optical Coherence Tomography*. New York, NY: Springer New York, 2009.

[33] C. Loudon and A. Tordesillas, “The Use of the Dimensionless Womersley Number to Characterize the Unsteady Nature of Internal Flow,” *J. Theor. Biol.*, vol. 191, no. 1, pp. 63–78, Mar. 1998.

[34] R. B. Bird, W. E. Stewart, and E. N. Lightfoot, “Transport Phenomena,” *J. Wiley*, 2007. .

[35] H. Blasius, “Forschungsarbeiten des Ver,” *Deutsch. Ing*, 1913.

[36] NEUTRIUM, “Discharge Coefficient for Nozzles and Orifices – Neutrium,” 2015. [Online]. Available: https://neutrium.net/fluid_flow/discharge-coefficient-for-nozzles-and-orifices/. [Accessed: 06-Apr-2017].

[37] *ISO 5167-1:2003 - Measurement of fluid flow by means of pressure differential devices inserted in circular cross-section conduits running full -- Part 1: General principles and requirements*. International Organization of Standards, 2003.

[38] *Measurement of Fluid Flow Using Small Bore Precision Orifice Meters*. American Society of Mechanical Engineers, 2003.

[39] H. E. Merritt and V. Pomper, “Hydraulic Control Systems,” in *Journal of Applied Mechanics*, vol. 35, no. 1, 1968, p. 200.

[40] L. D. Landau and E. M. Lifshitz, *Fluid Mechanics*, vol. 6, no. 1. 1987.

[41] J. Blackburn, “Fluid power control,” *The MIT Press*, 1969.

[42] G. E. Totten and V. J. de. Negri, *Handbook of hydraulic fluid technology*. CRC Press, 2012.

[43] R. E. Marx, “Platelet-rich plasma (PRP): what is PRP and what is not PRP?,” *Implant Dent.*, vol. 10, no. 4, pp. 225–228, 2001.

[44] R. E. Marx, “Platelet-rich plasma: evidence to support its use,” *J. Oral Maxillofac. Surg.*, vol. 62, no. 4, pp. 489–496, Apr. 2004.

[45] N. Circulation, “Role of Platelet Activation and Fibrin Formation in Thrombogenesis,” vol. X, no. 0.

[46] T. Kragh, J. Schaller, U. Kertzscher, K. Affeld, A. Reininger, and M. Spannagl, “Platelet adhesion , aggregation , and embolism on artificial surfaces in non - parallel blood flow,” pp. 155–167, 2015.

[47] K. K. Woronzoff-Dashkoff, “The wright-giemsa stain. Secrets revealed.,” *Clin. Lab. Med.*, vol. 22, no. 1, pp. 15–23, Mar. 2002.

[48] J. Loscalzo, M. Fisch, R. I. Handin, J. Harsfalvi, D. Wilson, and R. Marchant, “Solution studies of the quaternary structure and assembly of human von Willebrand factor.,” *Biochemistry*, vol. 24, no. 16, pp. 4468–75, Jul. 1985.